

**THE EFFECTS OF WAVE GROUPS ON THE NONLINEAR SIMULATION OF  
SHIP MOTION IN RANDOM SEAS**

A Thesis

by

JEFFREY A. RICHER

Submitted to the Office of Graduate Studies of  
Texas A&M University  
in partial fulfillment of the requirements for the degree of

MASTER OF SCIENCE

December 2005

Major Subject: Ocean Engineering

**THE EFFECTS OF WAVE GROUPS ON THE NONLINEAR SIMULATION OF  
SHIP MOTION IN RANDOM SEAS**

A Thesis

by

JEFFREY A. RICHER

Submitted to the Office of Graduate Studies of  
Texas A&M University  
in partial fulfillment of the requirements for the degree of

MASTER OF SCIENCE

Approved by:

Chair of Committee,  
Committee Members,

Head of Department,

Cheung Hun Kim  
Robert E. Randall  
Achim Stoessel  
David V. Rosowsky

December 2005

Major Subject: Ocean Engineering

**ABSTRACT**

The Effects of Wave Groups on the Nonlinear Simulation of Ship Motion in Random  
Seas. (December 2005)

Jeffrey A. Richer, B.S., Lehigh University

Chair of Advisory Committee: Dr. Cheung Hun Kim

Historically, the analysis of ship motion and loading responses has been performed in the frequency domain with both linear response amplitude operators and wave energy density spectra. This method, therefore, did not account for the nonlinear nature of waves. A more precise method is to obtain the response in the time domain, processing non-linear wave data with a linear response amplitude operator. Since the input is non-linear, even though the system is linear, the output will also be non-linear. This resultant data can then be used to generate a more accurate design of seaworthy vessels. Furthermore the linear frequency domain method does not account for the presence or effects of wave groups. This study shows the improved accuracy in the response obtained by accounting for non-linearities and furthermore indicates that wave groups affect the vertical relative motion of a moored ship (zero-speed).

## **DEDICATION**

To the Lord Jesus for his blessings on my life, to my Wife who kept me motivated, and  
the US Navy for getting me here

## ACKNOWLEDGEMENTS

This research was conducted at Texas A&M University and was supported by the Department of Civil Engineering, Texas A&M University through the Texas Engineering Experiment Station (TEEX).

I would like to thank my Chair, Dr. C. H. Kim, for his trust in my capabilities and instructing me in hydrodynamics, statistics, and naval architecture, without which my ability to perform this research would not have been possible. I would also like to thank Dr. Robert Randall; his experience and wisdom kept me on track and Dr. Achim Stoessel for agreeing to help out yet another Ocean Engineering student.

I also wish to thank my fellow classmates and friends for their active help and contributions: Mr. Rajith Padmanabhan, without whom none of my programs would have worked, Mr. Adam Adil, for breaking the ice on this topic, and Dr. Nungsoo Kim, whose mastery of computer programming ensured my data was accurate.

Special thanks to my family for always supporting me, even when the creative machine was jammed.

## TABLE OF CONTENTS

	Page
ABSTRACT.....	iii
DEDICATION.....	iv
ACKNOWLEDGEMENTS.....	v
TABLE OF CONTENTS.....	vi
LIST OF FIGURES.....	viii
LIST OF TABLES.....	xi
INTRODUCTION.....	1
A background into ship modeling weaknesses.....	1
The Universal Nonlinear Input Output model as a solution.....	4
THE UNIOM MODEL.....	6
Input spectrum generation.....	6
RAO generation by strip theory.....	7
ANALYSIS.....	11
Linear analysis.....	11
Comparison analysis.....	12
Wave group inspection.....	13
ANALYSIS RESULTS.....	15
Case 1: $H_S = 3$ m.....	17
Case 2: $H_S = 4$ m.....	21
Case 3: $H_S = 6$ m.....	25
Case 4: $H_S = 7$ m.....	29
Case 5: $H_S = 9$ m.....	33
Case 6: $H_S = 11$ m.....	37
CONCLUSIONS.....	41

	Page
REFERENCES.....	44
APPENDIX A.....	46
VITA.....	52

## LIST OF FIGURES

FIGURE	Page	
1	Comparisons of the theoretical RAO (dashed line) with measured RAOs for wave A – $H_s$ at 2.3% of the destroyer length, wave B – $H_s$ at 6.1% of the destroyer length and wave C – $H_s$ at 9.3% of the destroyer length for a constant Froude number (constant speed).....	2
2	Comparisons of the response spectrum using the ITTC input spectrum and the theoretical RAO and measured RAO for wave C – $H_s$ at 9.3% of the destroyer length .....	3
3	Time series random wave $X(t)$ , first order response $Y1(t)$ , second order response $Y2(t)$ , third-order response $Y3(t)$ , and the resultant response $Y(t)$ ...	4
4	Relative motion RAO used for each significant wave height.....	16
5	Wave profile measured amidships for $H_s = 3$ m.....	17
6	Wave profile at station 1 for $H_s = 3$ m.....	18
7	Relative motion profile at station 1 for $H_s = 3$ m.....	19
8	Comparison of the linear (theoretical) and nonlinear (experimental) input wave for $H_s = 3$ m.....	20
9	Comparison of the linear (theoretical) and nonlinear (experimental) relative motion profile for $H_s = 3$ m.....	20
10	Wave profile measured amidships for $H_s = 4$ m.....	21
11	Wave profile at station 1 for $H_s = 4$ m.....	22
12	Relative motion profile at station 1 for $H_s = 4$ m.....	23
13	Comparison of the linear (theoretical) and nonlinear (experimental) input wave for $H_s = 4$ m.....	24
14	Comparison of the linear (theoretical) and nonlinear (experimental) relative motion profile for $H_s = 4$ m.....	24
15	Wave profile measured amidships for $H_s = 6$ m.....	25



FIGURE	Page
16 Wave profile at station 1 for $H_s = 6$ m.....	26
17 Relative motion profile at station 1 for $H_s = 6$ m.....	27
18 Comparison of the linear (theoretical) and nonlinear (experimental) input wave for $H_s = 6$ m.....	28
19 Comparison of the linear (theoretical) and nonlinear (experimental) relative motion profile for $H_s = 6$ m.....	28
20 Wave profile measured amidships for $H_s = 7$ m.....	29
21 Wave profile at station 1 for $H_s = 7$ m.....	30
22 Relative motion profile at station 1 for $H_s = 7$ m.....	31
23 Comparison of the linear (theoretical) and nonlinear (experimental) input wave for $H_s = 7$ m.....	32
24 Comparison of the linear (theoretical) and nonlinear (experimental) relative motion profile for $H_s = 7$ m.....	32
25 Wave profile measured amidships for $H_s = 9$ m.....	33
26 Wave profile at station 1 for $H_s = 9$ m.....	34
27 Relative motion profile at station 1 for $H_s = 9$ m.....	35
28 Comparison of the linear (theoretical) and nonlinear (experimental) input wave for $H_s = 9$ m.....	36
29 Comparison of the linear (theoretical) and nonlinear (experimental) relative motion profile for $H_s = 9$ m.....	36
30 Wave profile measured amidships for $H_s = 11$ m.....	37
31 Wave profile at station 1 for $H_s = 11$ m.....	38
32 Relative motion profile at station 1 for $H_s = 11$ m.....	39
33 Comparison of the linear (theoretical) and nonlinear (experimental) input wave for $H_s = 11$ m.....	40

FIGURE	Page
34 Comparison of the linear (theoretical) and nonlinear (experimental) relative motion profile for $H_s = 11$ m.....	40
35 Most probable peak response for linear (theoretical) and nonlinear (experimental) data.....	42

**LIST OF TABLES**

TABLE		Page
1	Wave profile file characteristics.....	12
2	Response due wave group time lag and comparison to wave height.....	43

## INTRODUCTION

The objective is to show that by taking non-linear data measured in the time domain, and processing it using a linear system, the resultant non-linear output will not only be more accurate but can be further inspected for the effects of wave groups. The processing technique is referred to as the Universal Nonlinear Input Output Model (UNIOM), the non-linear input data will come from wave records, and the linear response amplitude operator (RAO) will come from linear strip theory. This work will then statistically compare the simulated relative motion for varying sea states created using both the conventional linear theory and that of the UNIOM model. Ultimately the time domain data will be then be inspected for the effects of wave groups, and the results tabulated.

### *A background into ship modeling weaknesses*

Historically ship motion modeling has been linear and in the frequency domain using the Linear Energy Spectral Method (Tupper, 1996) defined as:

$$U_{yy} = U_{xx} |RAO|^2 \quad (1)$$

where:

$U_{yy}$  = the linear response spectrum  
 $U_{xx}$  = the linear input spectrum  
 RAO = linear response amplitude operator

Dalzell (1962) and Cummins (1973) showed that as the operational sea states and velocities of a US Sumner Class destroyer increased the RAO decreased (see Fig. 1). This was due to the non-linearity of the waves that was NOT being considered by the linear system.

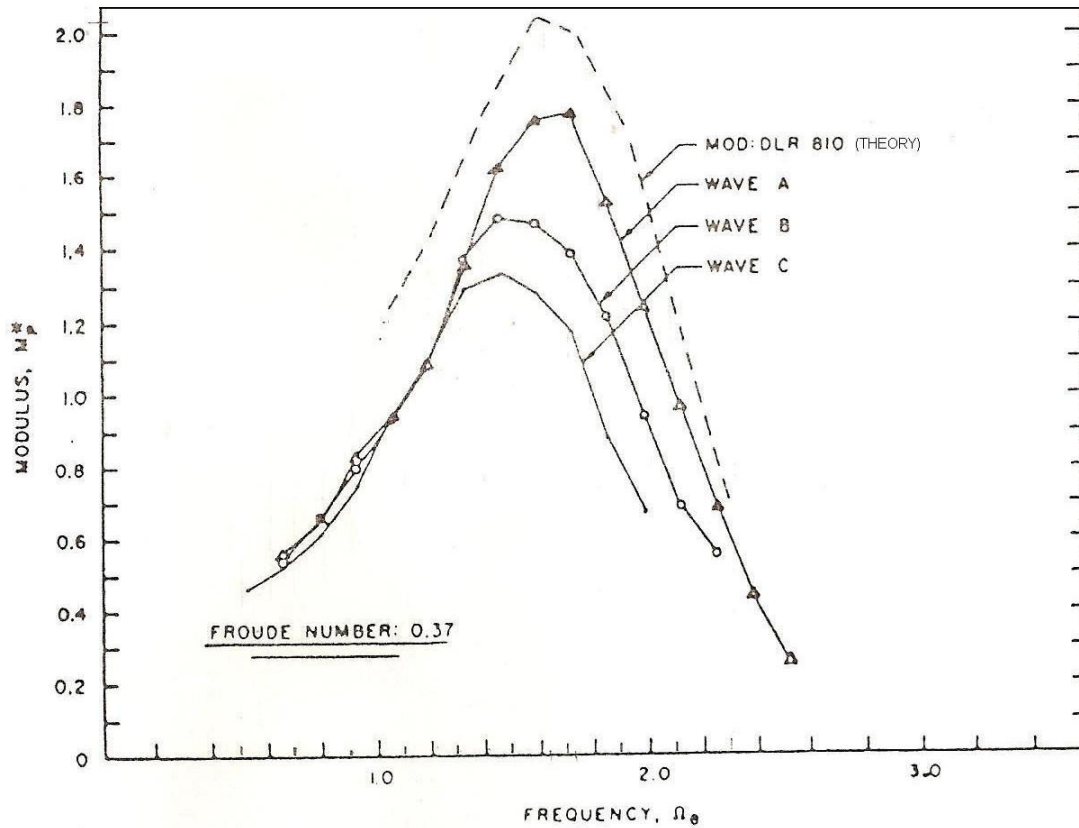


Fig. 1. Comparisons of the theoretical RAO (dashed line) with measured RAOs for wave A –  $H_s$  at 2.3% of the destroyer length, wave B –  $H_s$  at 6.1% of the destroyer length and wave C –  $H_s$  at 9.3% of the destroyer length for a constant Froude number (constant speed) (Dalzell 1962).

Since Dalzell's study showed that as the RAOs decrease, the sea states increase, using equation 1,  $U_{yy}$  will also decrease as the sea states increase (see Fig. 2). The overall result is that the actual response spectrum is less than theoretical response.

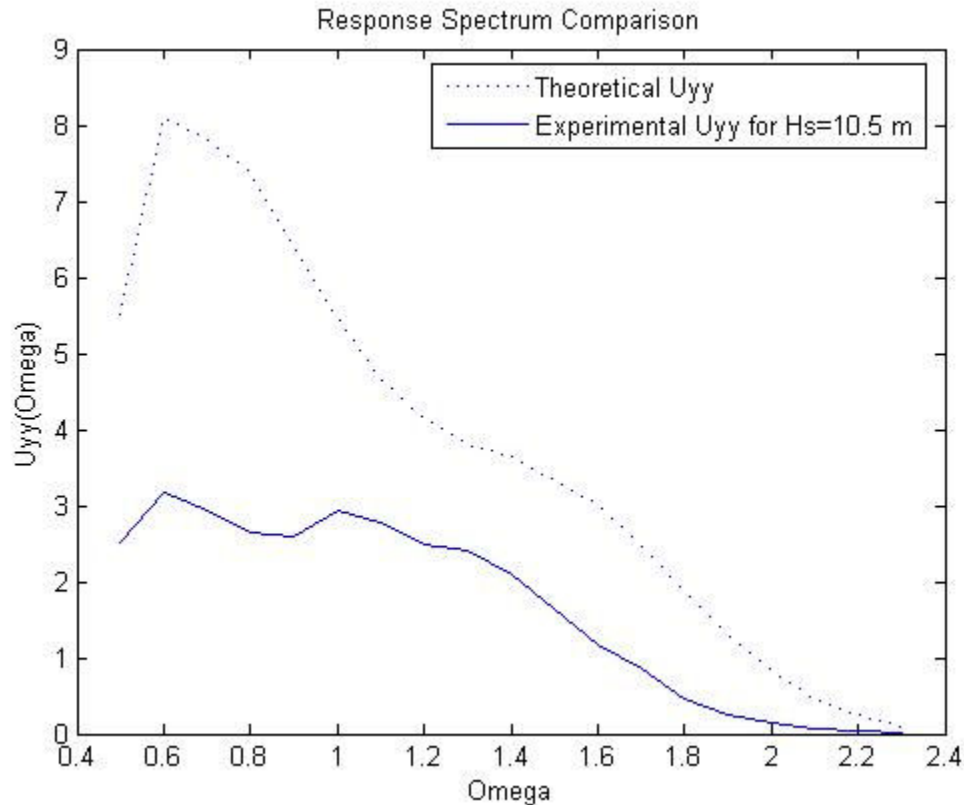


Fig. 2. Comparisons of the response spectrum using the ITTC input spectrum and the theoretical RAO and measured RAO for wave C –  $H_s$  at 9.3% of the destroyer length.

Dalzell's analysis showed that by holding the input spectrum constant, and since the measured RAO was less than the theoretical RAO, the actual response would be less. Adil (2004) showed in his study that by using UNIOM, which holds the RAO constant, and varies the input spectrum, the resultant calculated response spectrum was also less than the theoretical response.

Furthermore Dalzell (1982) showed that as the order of wave increased from first to second and third, that wave groups had a significant effect on response (see Fig. 3).

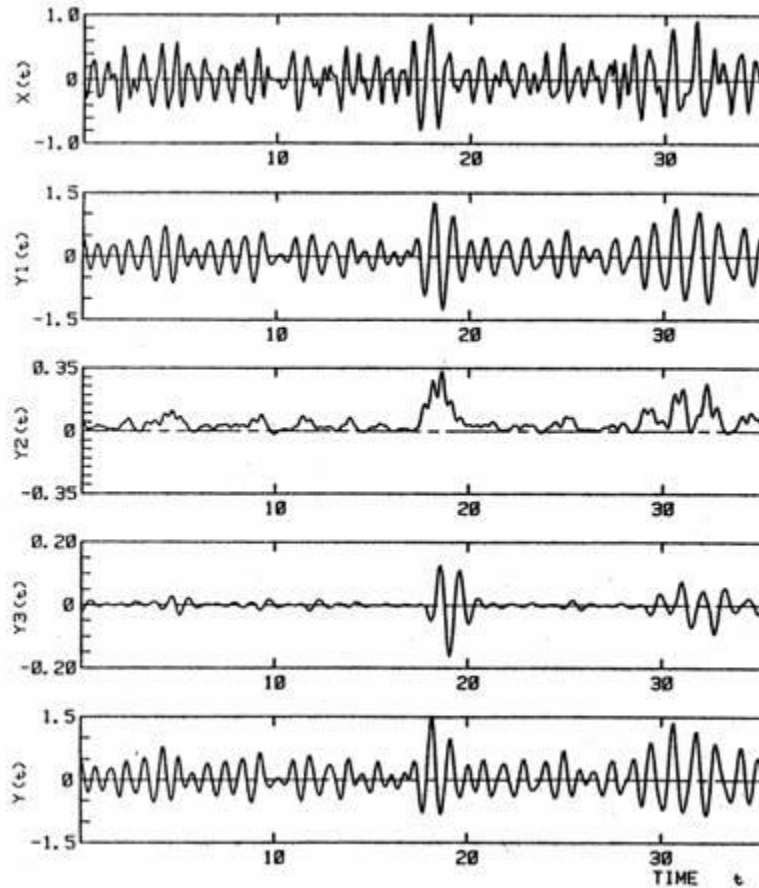


Fig. 3. Time series random wave  $X(t)$ , first order response  $Y1(t)$ , second order response  $Y2(t)$ , third-order response  $Y3(t)$ , and the resultant response  $Y(t)$  (trial test by Dalzell, 1982).

### *The Universal Nonlinear Input Output Model as a solution*

The Universal Nonlinear Input Output Model (UNIOM) is able to address the short comings of the Linear Energy Spectral Method, and is defined as

$$\text{Rel}(t) = \sum_{j=1} |A_j| |RAO| e^{i(\omega_j t - \phi_j - \varepsilon_j)} \quad (2)$$

where:

$\text{Rel}(t)$  = the response motion in the time domain  
 $A_j$  = the nonlinear input amplitude in the frequency domain  
 $RAO$  = linear response amplitude operator

$\omega_j$  = the frequency  
 $\phi_j$  = the phase of the amplitude  
 $\varepsilon_j$  = the phase of the RAO

This method takes real nonlinear wave data generated in a wave tank (as opposed to linear Gaussian random wave data generated from and spectrum generated according to significant wave height), and processes it with a linear RAO, which is generated by performing a linear strip theory analysis on a ship. The result is non-linear output of how the ship performs.

Furthermore since this output is in the time domain, the response profile can be compared with the input wave profile to inspect for the effects of wave groups.



## THE UNIOM MODEL

The present study will use nonlinear model wave profile data from the Korean Research Institute of Ship and Ocean Engineering (KRISO). The wave profiles were generated in a wave tank using both the ITTC and JONSWAP spectrum for varying significant wave heights. Although the wave maker used linear spectrums to generate the waves, the resultant profiles in the wave tank itself display nonlinear effects. For this reason the KRISO data is considered nonlinear.

The nonlinear KRISO data will then be processed with a linear relative motion RAO for an SL-7 container ship computed using two dimensional strip theory. The process simply involves multiplication in the time domain (accounting for phase angles), and therefore does not eliminate any of the nonlinearities of the input data. Simply stated, since the input data is nonlinear, the output data must also be nonlinear.

### *Input spectrum generation*

The input spectrums for the UNIOM model come from the transformation of the time domain KRISO data into the frequency domain using the Fourier Transform. The first step of the transformation is to generate the Fourier Coefficients for a given set of time domain data  $\eta(t)$  of total time length T, from the following equation:

$$\eta(t) = A_0 + \sum_{n=1}^{\infty} (A_n \cos \omega_n t + B_n \sin \omega_n t) \quad (3)$$

where:

$$\begin{aligned} \omega_1 &= 2\pi/T \text{ and } f = 1/T = \Delta t && \text{the fundamental frequency} \\ \omega_n &= n \omega_1 \text{ and } f = n f_1 && \text{the } n^{\text{th}} \text{ harmonic} \end{aligned}$$

For the zero mean case:

$$\eta(t) = \text{Re} \sum_{n=1}^{\infty} (A_n - iB_n) e^{i\omega_n t} \quad (4)$$

For the present study the Fourier Transform is performed using the FFT command in MATLAB. The resultant array generated contains  $A_0$  as the first element and the  $n$ th  $A$  (real) and  $B$  (imaginary) coefficients as the subsequent elements. It must be noted that the MATLAB FFT routine does not consider the time interval resulting in  $N$  pairs coefficients. For this reason each value of the array needs to be divided by  $N$ . Furthermore, since the values in the array beyond the  $N/2^{\text{th}}$  element are the symmetrical counterpart to the first  $N/2$  values, they can be eliminated. From the resultant  $N/2$  elements, the amplitudes and phase angles can be computed.

#### *RAO generation by strip theory*

The relative motion RAO for the SL-7 container ship is created using strip theory (Kim et al, 1980). Because the strip theory computations are extensive, in the early 1980's Dr. C.H. Kim developed two computer programs to compute the RAO's. SHMB5 computes the heave, pitch and roll RAO's and generates a relative motion array that is used by PRDMR5 to compute the relative motion RAO.

In this program the strips are modeled at 13 stations (Stations 1, 1.5, 2, 3, 4, 5, 6, 7, 8, 9, 10, 10.5, and 11). At each of these stations the program uses the Frank Close Fit method which applies the free surface and body boundary conditions of zero pressure and no normal flow respectively to determine the strength of singularities on the surface of the strip. From these singularities the program generates parameters for added mass, damping, and wave excitation. The results are then integrated along the length of the hull, coupling heave and pitch, as well as sway, roll, and yaw to generate coefficients for the ship as whole. With these values the program computes the heave, surge, sway, roll,

pitch and yaw motions. Once these motions are obtained, the computer then generates the relevant forces and response spectra.

To simplify, SHMB5 is solving the equations of motion based on Newton's second law of dynamics for six degrees of freedom. In a right handed coordinate system with the origin at the ships center of gravity, the basic equation is:

$$\sum_{j=1}^6 \{ (M_{kj} + A_{kj}) \ddot{x}_j + B_{kj} \dot{x}_j + C_{kj} x_j \} = X_k$$

for  $k = 1, 2, 3, 4, 5, 6$

(5)

where:

- M = mass
- A = added mass
- B = damping coefficient
- C = stiffness coefficient
- $x_j$  = amplitude of harmonic oscillations in direction  $j$
- $\dot{\phantom{x}}$  = first derivative - velocity
- $\ddot{\phantom{x}}$  = second derivative - acceleration
- $X_k$  = force
- $k = 1, 3,$  and  $5$ : Coupled surge, heave, and pitch
- $k = 2, 4,$  and  $6$ : Coupled sway, roll, and yaw motions

Furthermore the ship is assumed to maintain its initial course at a constant speed subjected to an oblique regular wave train, whose equation is given as:

$$h = ae^{i(\nu y \cos \mu + \nu x \sin \mu - \omega t)}$$
(6)

with

$$\omega = \omega_0 - \nu U \cos \mu$$
(7)

where:

- h = wave elevation
- a = wave amplitude
- $\nu$  = wave number
- y = ship's coordinate
- $\mu$  = wave incidence
- U = ship speed

The ship motions in response to this wave are then solved using the coupled linear equations:

$$\begin{pmatrix} \{ (B_{\zeta\zeta} - \omega^2 M_{\zeta\zeta}) - i\omega N_{\zeta\zeta} \} \{ (B_{\psi\zeta} - \omega^2 M_{\psi\zeta}) - i\omega N_{\psi\zeta} \} \\ \{ (B_{\zeta\psi} - \omega^2 M_{\zeta\psi}) - i\omega N_{\zeta\psi} \} \{ (B_{\psi\psi} - \omega^2 M_{\psi\psi}) - i\omega N_{\psi\psi} \} \end{pmatrix} \begin{pmatrix} \zeta / a \\ \psi / a \end{pmatrix} = \begin{pmatrix} F_{\zeta} / a \\ F_{\psi} / a \end{pmatrix} \quad (8)$$

$$\begin{pmatrix} (-\omega^2 M_{\eta\eta} - i\omega N_{\eta\eta})(-\omega^2 M_{\chi\eta} - i\omega N_{\chi\eta})(-\omega^2 M_{\phi\eta} - i\omega N_{\phi\eta}) \\ (-\omega^2 M_{\eta\chi} - i\omega N_{\eta\chi})(-\omega^2 M_{\chi\chi} - i\omega N_{\chi\chi})(-\omega^2 M_{\phi\chi} - i\omega N_{\phi\chi}) \\ (-\omega^2 M_{\eta\phi} - i\omega N_{\eta\phi})(-\omega^2 M_{\chi\phi} - i\omega N_{\chi\phi})(-\omega^2 M_{\phi\phi} - i\omega N_{\phi\phi}) \end{pmatrix} \begin{pmatrix} \eta / a \\ \chi / a \\ \phi / a \end{pmatrix} = \begin{pmatrix} F_{\eta} / a \\ F_{\chi} / a \\ F_{\phi} / a \end{pmatrix} \quad (9)$$

where the time factor  $e^{-i\omega t}$  is eliminated.

For each of these matrix equations, in the first matrix, B, M, and N, represent restoring, inertial and damping forces per unit displacement, acceleration, and velocity respectively. The inertial M in the diagonal elements represent virtual mass. Each off diagonal elements is a cross coupling term whose first subscript represents the mode of motion, and second represents mode of induced force. The second matrix contains the RAO, and the third matrix contains the wave exciting forces.

With these equations solved, PRDMM5 uses these data, as well as the hydrodynamic pressure distribution along the waterline, to solve for the relative vertical motion of the ship.

The wave elevation due to hydrodynamic pressure (dynamic swell up) is given as:

$$p_{DS}/\rho g a = (p_1 + p_2 + p_3)/\rho g a \quad (10)$$

The vertical motion of the at-rest waterline  $z_{\pm}$  is:

$$z_{\pm} = \zeta - x\psi - iU\psi/\omega \pm B(x)\phi/2 \quad (11)$$

where  $\pm$  indicates the port and starboard sides of the hull, and  $B(x)/2$  is the half section beam in the waterplane.

The vertical relative motion of the ship, therefore is the difference between the dynamic swell up, and the vertical motion of the at rest water line:

$$r_{\pm}/a = p_{DS}/\rho g a - z_{\pm}/a \quad (12)$$

## ANALYSIS

In order to validate the efficacy of the experimental UNIOM results for generating the response, the results are compared to the results of the theoretical linear energy spectral method for six different significant wave heights.

### *Linear analysis*

The input spectrums for the linear analysis come from one of two industry standard sources, the International Towing Tank Conference (ITTC), or a modified Joint North Sea Wave Project (JONSWAP).

For lower sea states, ( $H_s = 3\text{m}$  and  $4\text{m}$ ) the present study uses a modified form of the Bretschneider spectrum recommended by the 15<sup>th</sup> International Towing Tank Conference of 1978 (ITTC, 1978). The Energy Density Spectrum is computed as:

$$S(\omega) = (A/\omega^5)\exp(-B/\omega^4) \quad (13)$$

where according to  $H_s$  (the significant wave height)  $T_1$  (the characteristic period):

$$A = 173H_s^2/T_1^4 \quad (14)$$

$$B = 691/T_1^4 \quad (15)$$

For higher sea states ( $H_s = 6\text{m}$ ,  $7\text{m}$ ,  $9\text{m}$ , and  $11\text{m}$ ), the present study uses a modified JONSWAP spectrum using two parameters (with 2 scaling parameters  $\gamma$  and  $\sigma$ )  $H_s$  and  $T_p$  (the peak period) (Lee and Bales, 1980):

$$S(\omega) = \frac{5}{16} H_s^2 \omega_m^4 \omega^{-5} \exp\left\{-1.25\left(\frac{\omega_m}{\omega}\right)^4\right\} (1 - 0.287 \ln \gamma) \gamma^{\exp\left[\frac{(\omega - \omega_m)^2}{2\sigma^2 \omega_m^2}\right]} \quad (16)$$

where:

$$\omega_m = (3/5)^{1/4} 2\pi/T \quad (17)$$

Once the input spectrums are generated, the response spectrums are calculated using equation 1.

### *Comparison analysis*

Now that the input spectrums for both the linear (theoretical) and nonlinear (experiment) scenarios, and the RAO's have been generated, and the resultant output spectrums have been calculated, the data is inspected for the frequencies of significance, and the insignificant high and low frequencies are eliminated. In the present study these frequencies are between 0.2 and 1.5. Finally a comparison can be made between the linear and nonlinear results.

For each of the significant wave heights used for the present study, the analysis is performed according to Table 1.

Table 1  
Wave profile file characteristics

Data No.	Sea State	Prototype		Model		$\gamma$	Comparison Spectrum
		Hs (m)	Tz/T <sub>1</sub> or T <sub>p</sub>	Hs (m)	Tz/ T <sub>1</sub> or T <sub>p</sub>		
#043	C1	3.0	8.0/11.26	0.055	1.079/1.519	1.0	ITTC
#042	A1	4.0	8.0/11.26	0.073	1.079/1.519	1.0	ITTC
#010	A2	6.0	9.5/12.09	0.109	1.281/1.630	1.5	JONSWAP
#014	B1	7.0	9.5/12.09	0.127	1.281/1.630	2.0	JONSWAP
#020	B2	9.0	10.0/12.73	0.164	1.348/1.717	2.5	JONSWAP
#028	B3	11.0	10.5/13.37	0.200	1.416/1.803	2.5	JONSWAP

So for example, KRISO used the ITTC spectrum to generate data set #043. This model wave profile in their tank has  $H_s = 0.055$  m, and  $T_z$  and  $T_1$  of 1.079 s and 1.519 s respectively. These data are then scaled to a prototype (real world)  $H_s$  of 3 m and  $T_z$  and  $T_1$  of 8.0 s and 11.26 s respectively. The comparison between UNIOM and the linear energy spectral method for this example will therefore be made between the nonlinear response from data set #043, and the ITTC spectrum for  $H_s = 3$  m and  $T_1 = 11.26$ .

Once the responses have been generated for both the nonlinear and linear scenarios, a comparison of each can be made using a Rayleigh Probability of Exceedence:

$$\Pr\{peaks \geq a\} = \exp(-a^2/2m_0) \quad 0 \leq a \leq \infty \quad (18)$$

where  $m_0$  is the variance of the energy density spectrum.

#### *Wave group inspection*

The KRISO data used for the present study is measured amidships of the SL-7 containership, and this wave profile is considered to be the reference wave for any analysis of any point on the ship's hull. SHMB5 and PRDMR5 compute the RAO for any one of the stations along the hull of the ship. Since the maximum vertical relative motion will occur at station one (due to both the heave and the pitch contributions), this study analyzes the results at this station. So the nonlinear vertical relative motion at station one is computed using the UNIOM equation, with the KRISO data set amidships, and the RAO computed for station 1.

In order for the comparison between the relative motion, and the input wave to be accurate, an accurate view of the wave profile at any given location on the ship's hull is needed. Since the KRISO data are recorded at a single fixed point in space, in order to



accurately represent the data at other points of the vessel, the dispersion of wave groups and wave group velocities must be considered. For the present study, the accuracy propagation by linear dispersion is accurate enough and is defined by:

$$\eta(t) = \sum A \cos(kx + \omega t + \Phi) \quad (19)$$

where:

$\eta(t)$  = the wave surface

$A$  = the wave amplitude from the amplitude spectrum

$k$  = the wave number

$x$  = the propagation distance (half the ship length for this study)

$\omega$  = wave frequency

$t$  = the propagation time

$\Phi$  = the wave phase angle

In the case of this study the KRISO data is propagated from amidships to station 1.

## ANALYSIS RESULTS

The results show that for all significant wave heights ( $H_s = 3\text{m}, 4\text{m}, 6\text{m}, 7\text{m}, 9\text{m}, 11\text{m}$ ), the probability exceedences of the theoretical input waves are less than those for the experimental data. This indicates the nonlinearity of the KRISO data. The probability of exceedences for the response profiles show that linear responses exceed the nonlinear responses, indicating that compared to the UNIOM model, the linear energy spectral method overestimates the relative motion of the SL-7 container ship.

Furthermore inspection of each scenario indicates that wave groups in the input data affect the relative motion response in that at select relative maxima in the water surface elevation profile (representing wave groups), there is a maximum in the response of the ship, following a slight time lag. However, detailed inspection of the wave groups is beyond the scope of the present study. Propagating the KRISO data from midship to station 1, the groups are subject to dispersion, and therefore difficult to identify specifically.

Figure 4 is the RAO for the SL-7 containership stationary (zero speed) in head seas.

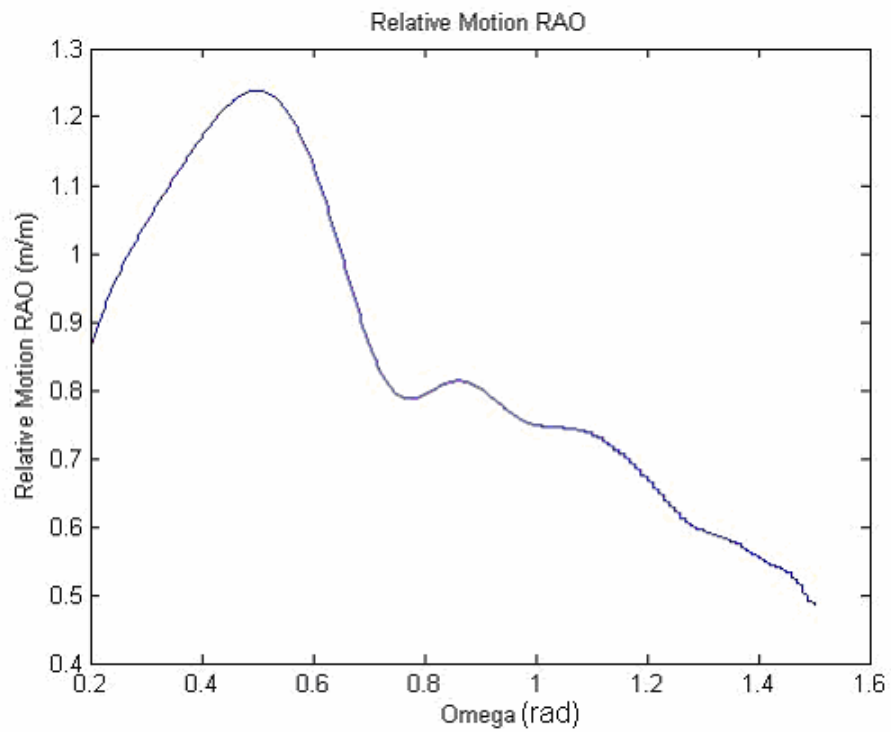


Fig. 4. Relative motion RAO used for each significant wave height.

Case 1:  $H_s = 3$  m

Figure 5 is the unpropagated KRISO data, which is propagated to station 1 in Figure 6. Note the peak of a group in the propagated KRISO data of 1.42 m at 316 s, 2.88 m at 460 s, and 2.24 m at 827 s (see Fig. 6). These groups then correspond to a response of 1.89 m at 327 s, 1.48 m at 483 s, and 2.22 at 866 s (see Fig. 7).

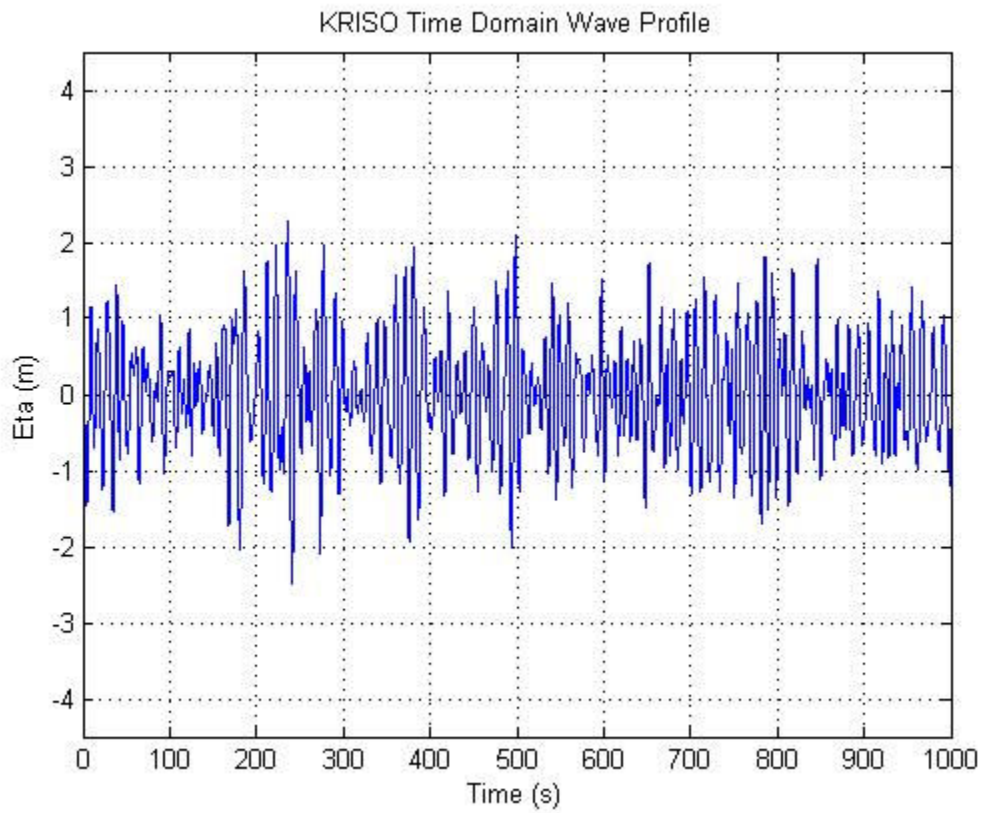


Fig. 5. Wave profile measured amidships for  $H_s = 3$  m.

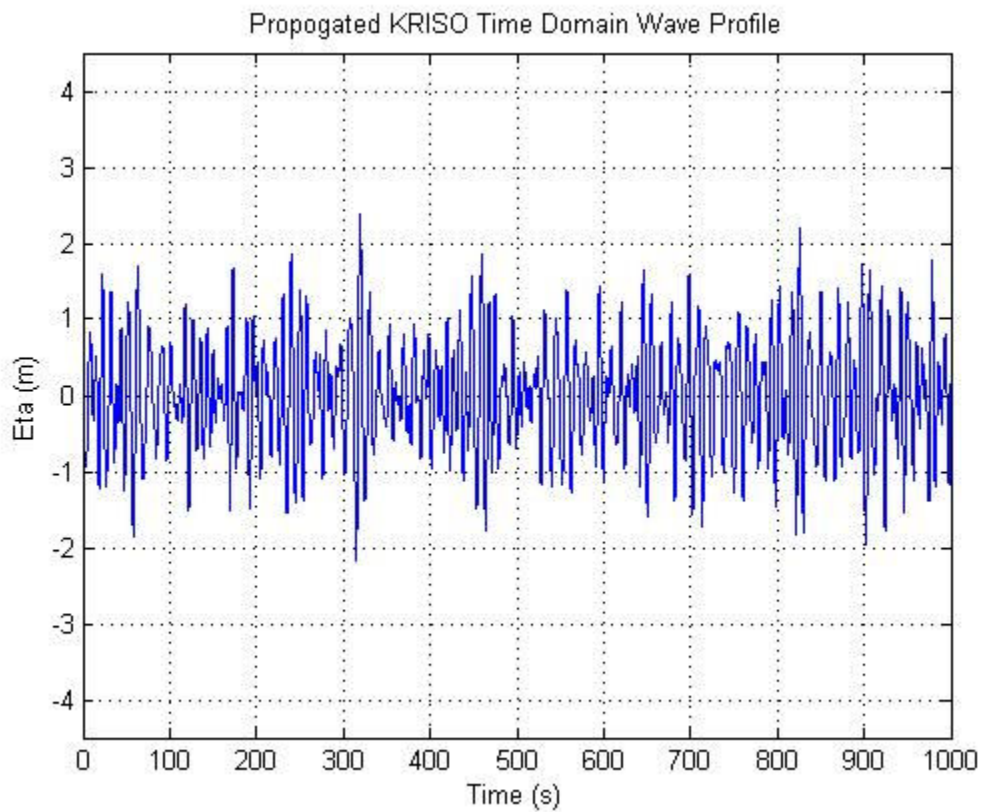


Fig. 6. Wave profile at station 1 for  $H_s = 3$  m.

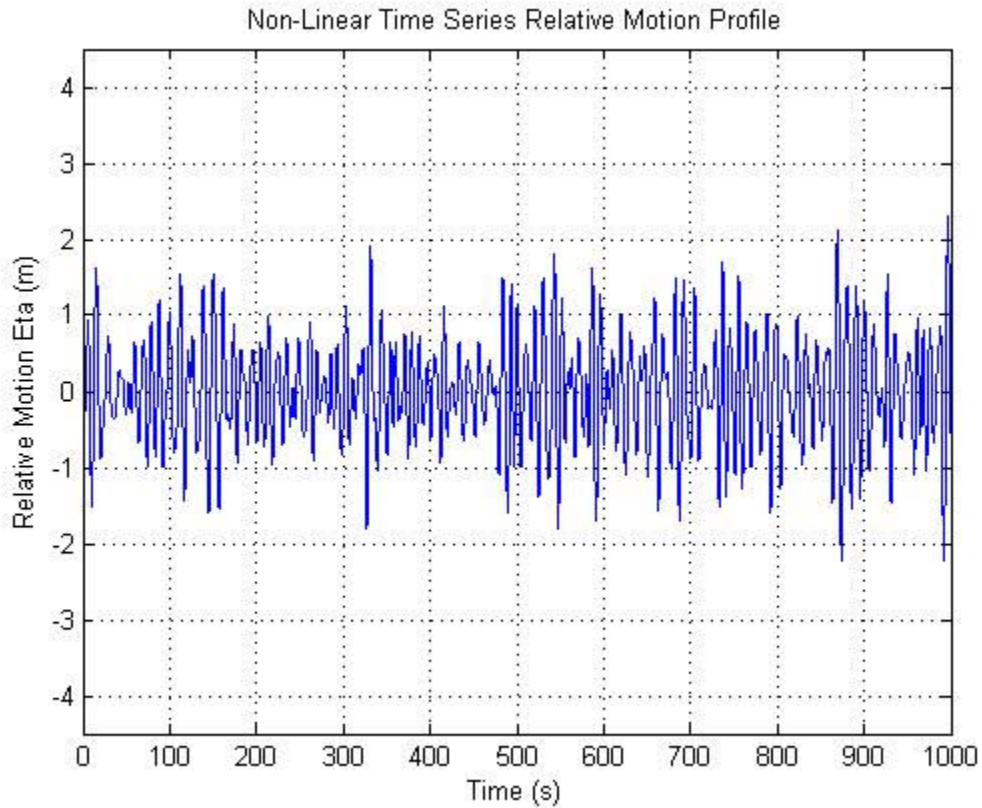


Fig. 7. Relative motion profile at station 1 for  $H_s = 3$  m.

Notice that for  $H_s = 3$  m the probability of exceedence curve for the linear model of the input wave matches that of the nonlinear fairly well. This indicates that for this significant wave height, that linear approximation is very close to nonlinear (see Fig. 8). However, in the response probability of exceedence curves, the nonlinear is less than that of the linear (see Fig. 9). This indicates that the linear theory is over approximating the nonlinear response.

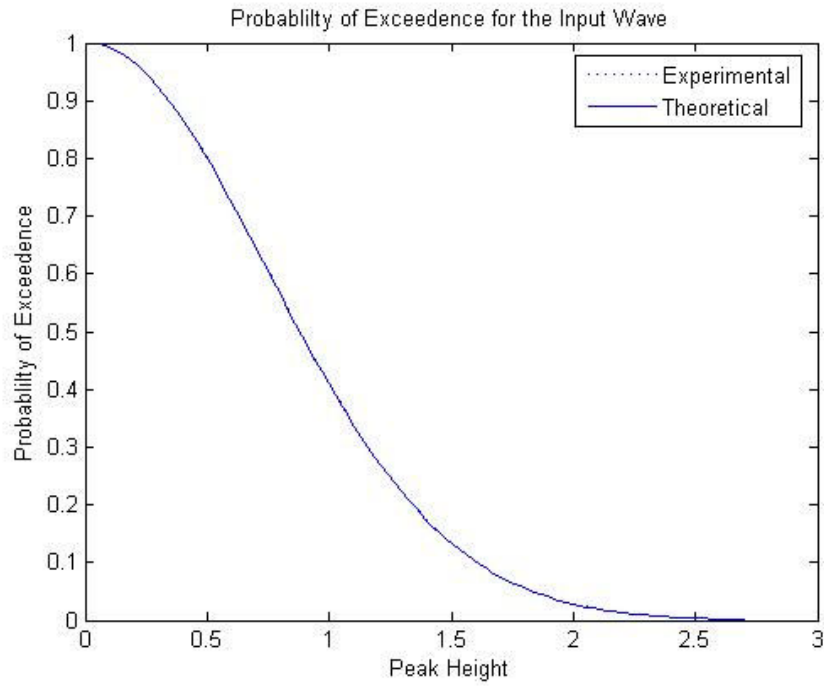


Fig. 8. Comparison of the linear (theoretical) and nonlinear (experimental) input wave for  $H_s = 3$  m.

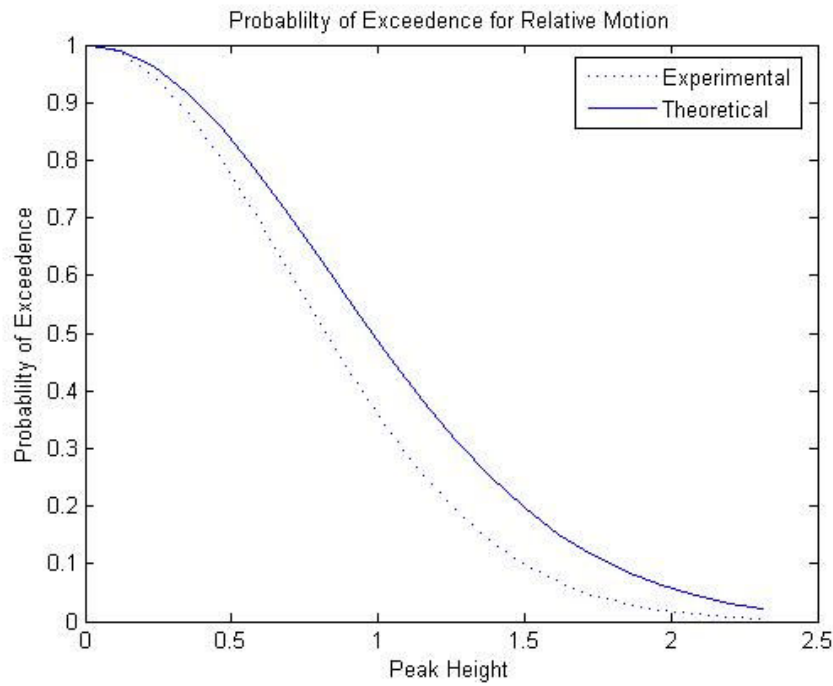


Fig. 9. Comparison of the linear (theoretical) and nonlinear (experimental) relative motion profile for  $H_s = 3$  m.

Case 2:  $H_s = 4$  m

Figure 10 is the unpropagated KRISO data, which is propagated to station 1 in Figure 11. Note the peak of a group in the propagated KRISO data of 3.00 m at 466 s, and another 3.00 m at 835 s (see Fig. 11). These groups then correspond to a response of 2.86 m at 477 s and also at 860 s (see Fig. 12).

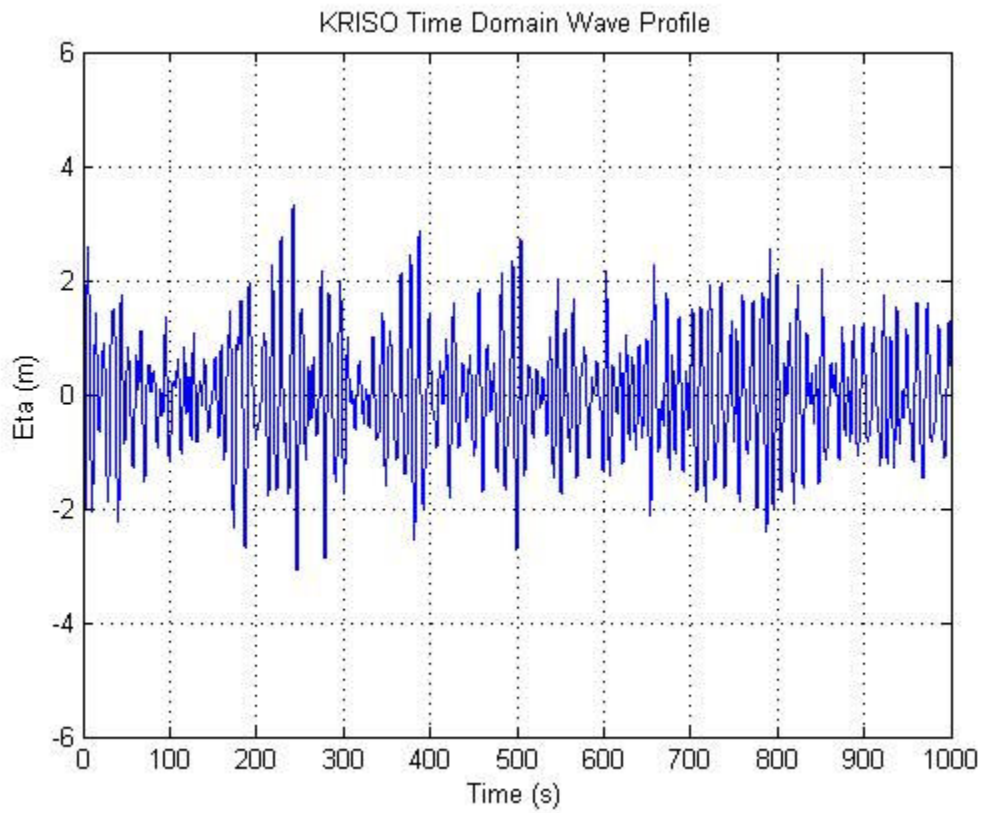


Fig. 10. Wave profile measured amidships for  $H_s = 4$  m.



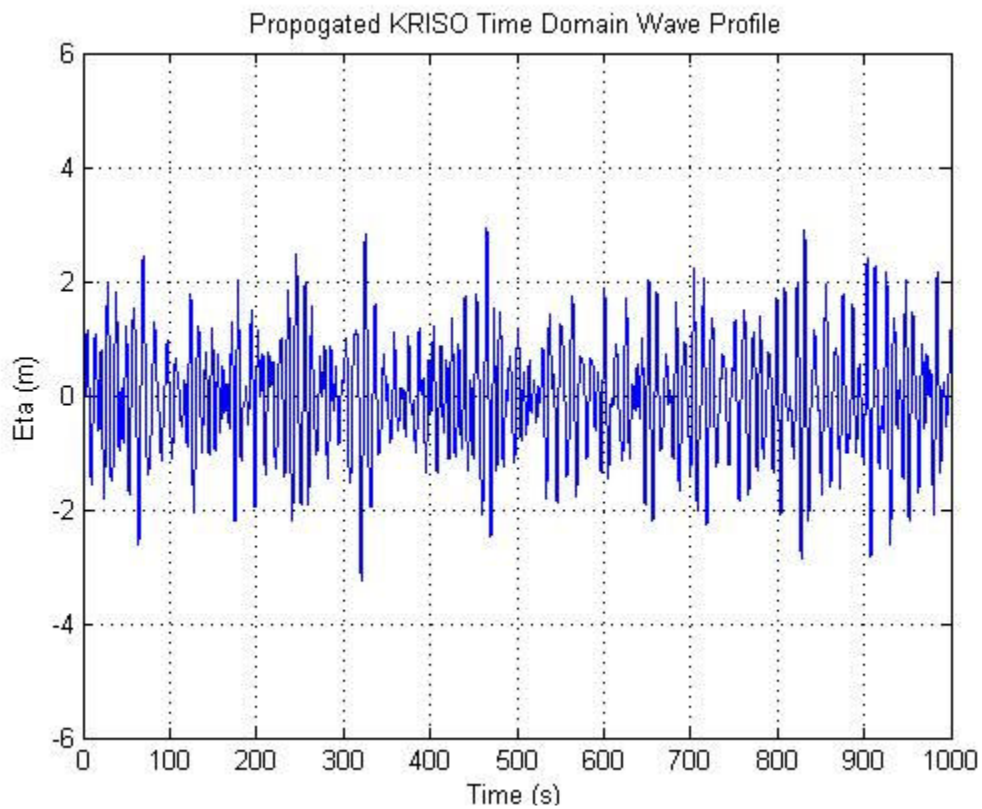


Fig. 11. Wave profile at station 1 for  $H_s = 4$  m.

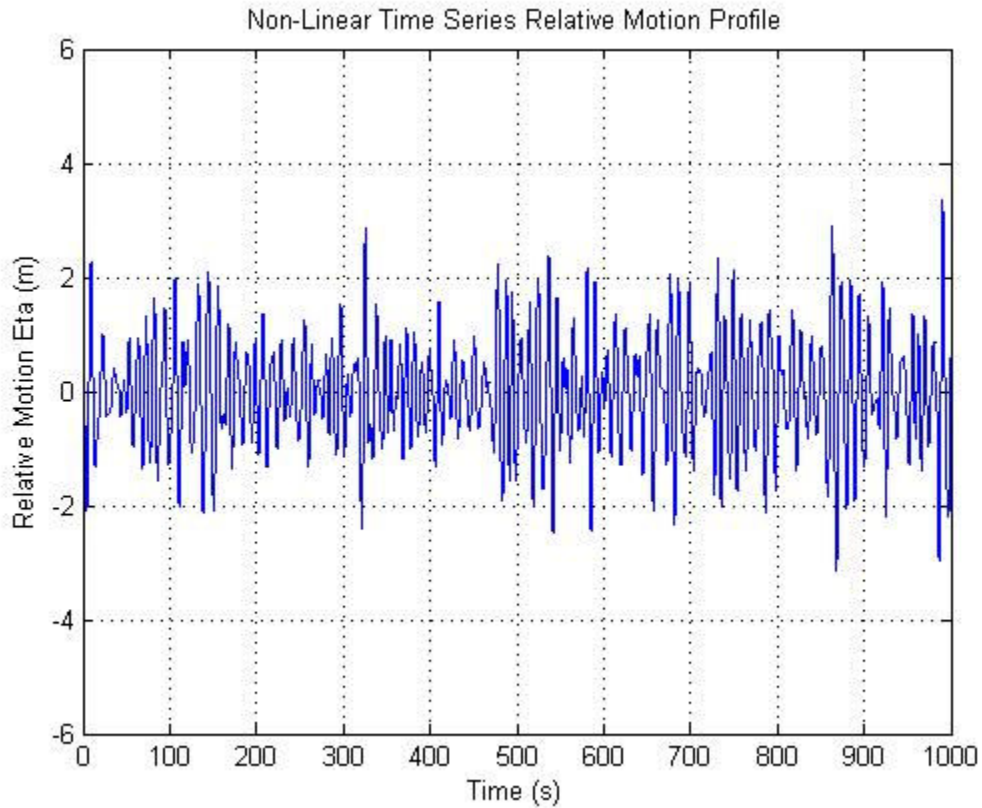


Fig. 12. Relative motion profile at station 1 for  $H_s = 4$  m.

Notice that for  $H_s = 4$  m the probability of exceedence curve for the linear model input wave is only slightly lower than that of the nonlinear. This again indicates that for low significant wave heights, that linear approximation is very close to nonlinear (see Fig. 13). However, in the response probability of exceedence curves, the nonlinear is less than that of the linear (see Fig. 14). This indicates that the linear theory is over approximating the nonlinear response.

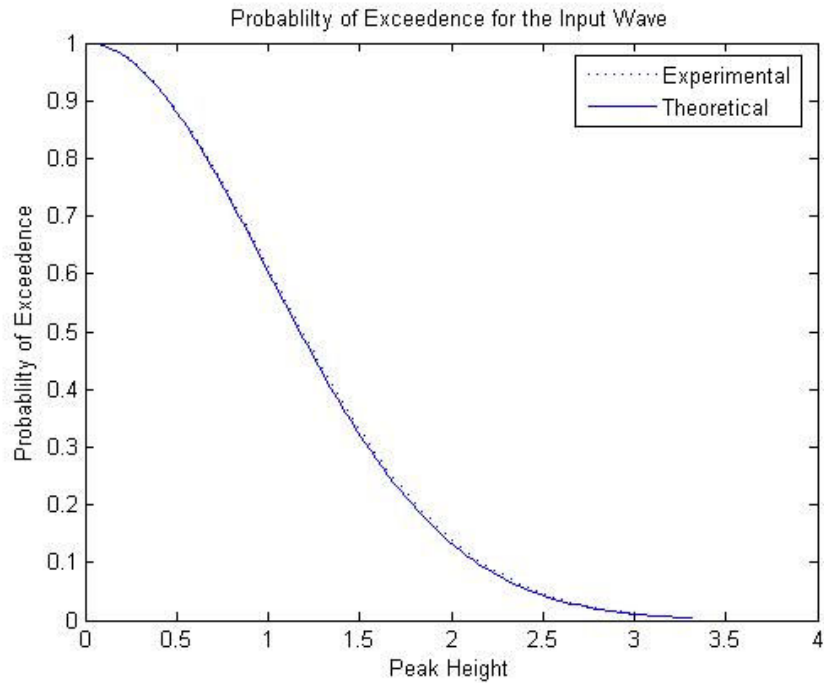


Fig. 13. Comparison of the linear (theoretical) and nonlinear (experimental) input wave for  $H_s = 4$  m.

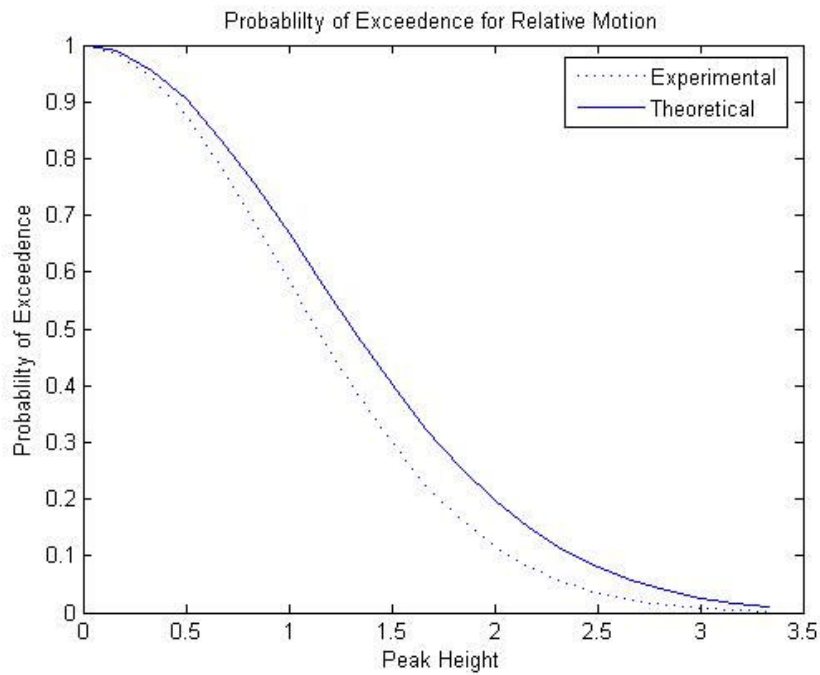


Fig. 14. Comparison of the linear (theoretical) and nonlinear (experimental) relative motion profile for  $H_s = 4$  m.

Case 3:  $H_s = 6\text{ m}$

Figure 15 is the unpropagated KRISO data, which is propagated to station 1 in Figure 16. Note the peak of a group in the propagated KRISO data of 4.47 m at 318 s (see Fig. 16). This group then corresponds to a response of 4.61 m at 330 s (see Fig. 17).

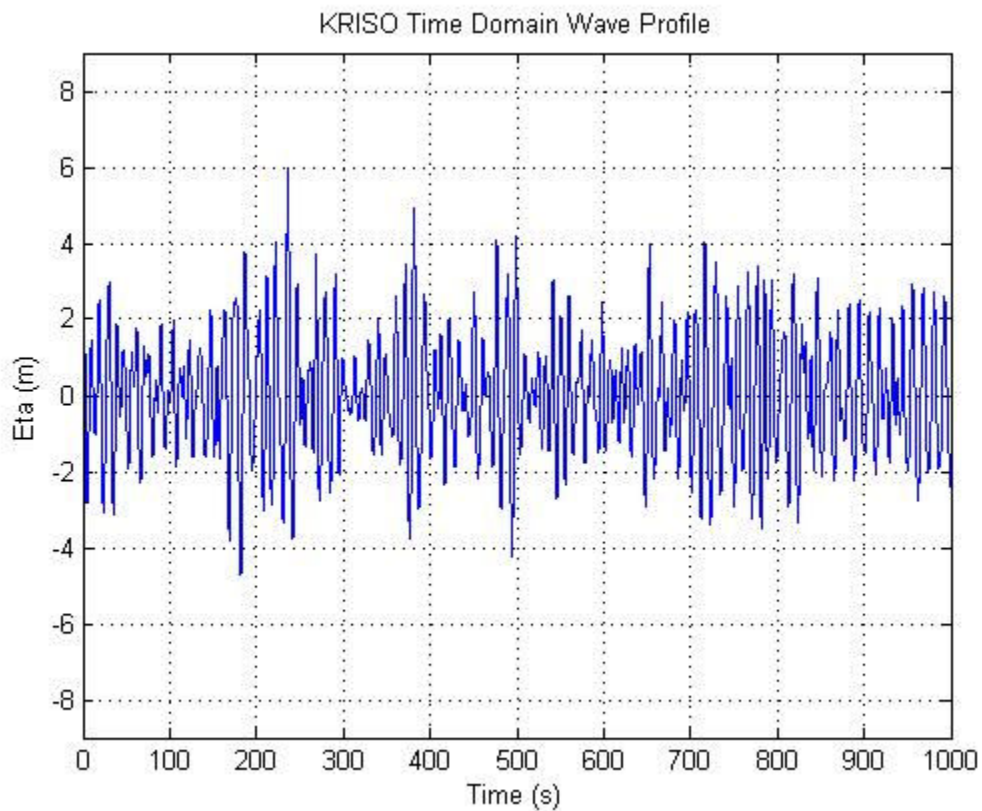


Fig. 15. Wave profile measured amidships for  $H_s = 6\text{ m}$ .

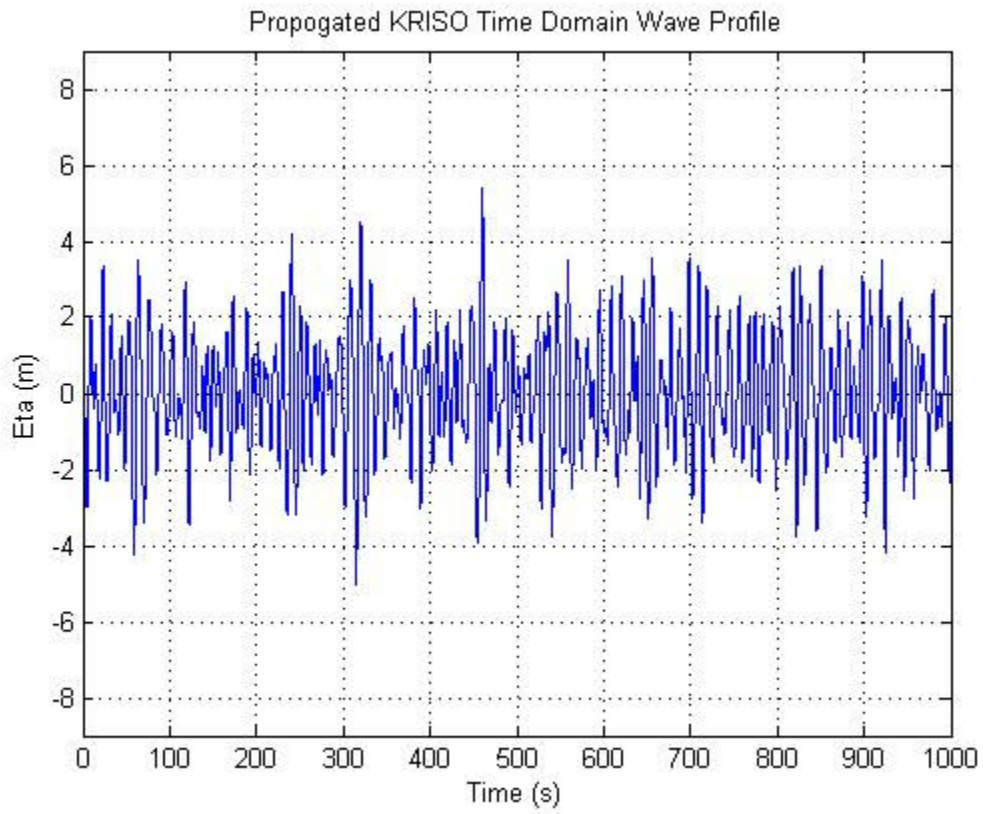


Fig. 16. Wave profile at station 1 for  $H_s = 6$  m.

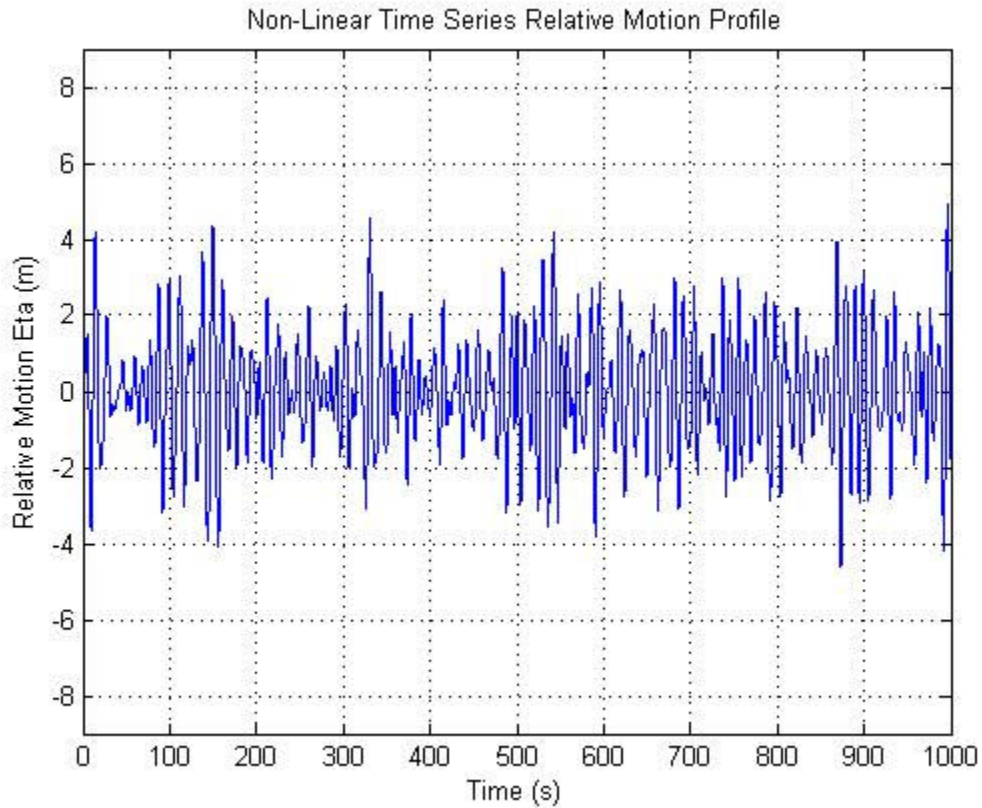


Fig. 17. Relative motion profile at station 1 for  $H_s = 6$  m.

Notice that for  $H_s = 6$  m the probability of exceedence curve for the linear model input wave is lower than that of the nonlinear. This indicates that as significant wave heights begin to increase, that nonlinearities begin to play a significant role in the modeling (see Fig. 18). Like in the lower sea states, in the response probability of exceedence curves, the nonlinear is less than that of the linear (see Fig. 19). This again indicates that the linear theory is over approximating the nonlinear response.

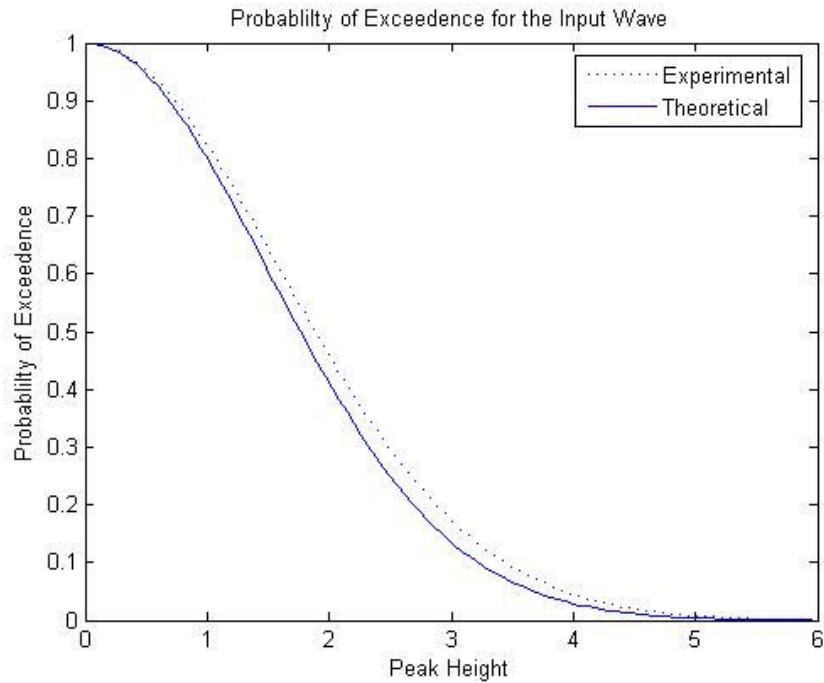


Fig. 18. Comparison of the linear (theoretical) and nonlinear (experimental) input wave for  $H_s = 6$  m.

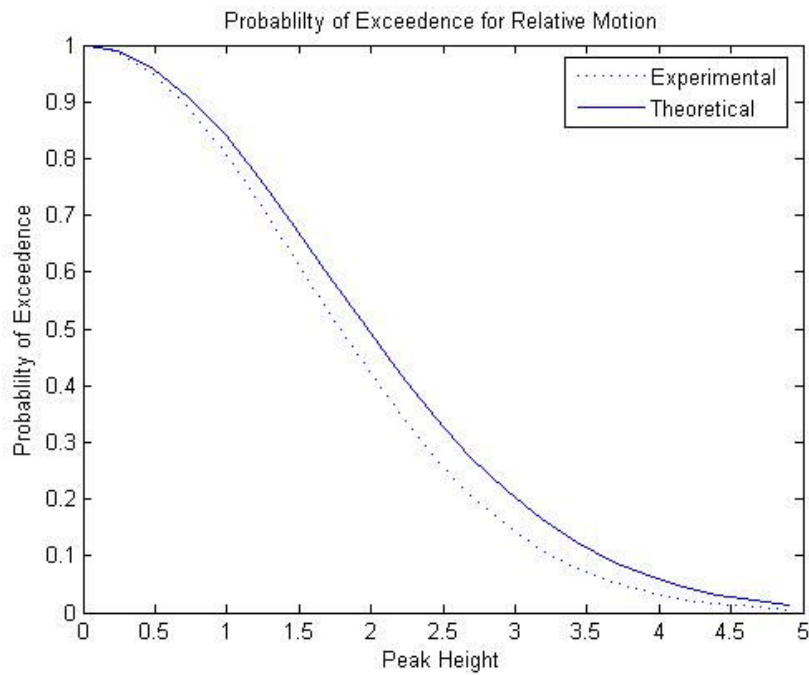


Fig. 19. Comparison of the linear (theoretical) and nonlinear (experimental) relative motion profile for  $H_s = 6$  m.

Case 4:  $H_s = 7\text{ m}$

Figure 20 is the unpropagated KRISO data, which is propagated to station 1 in Figure 21. Note the peak of a group in the propagated KRISO data of 5.20 m at 310 s (see Fig. 21). This group then corresponds to a response of 5.23 m at 340 s (see Fig. 22).

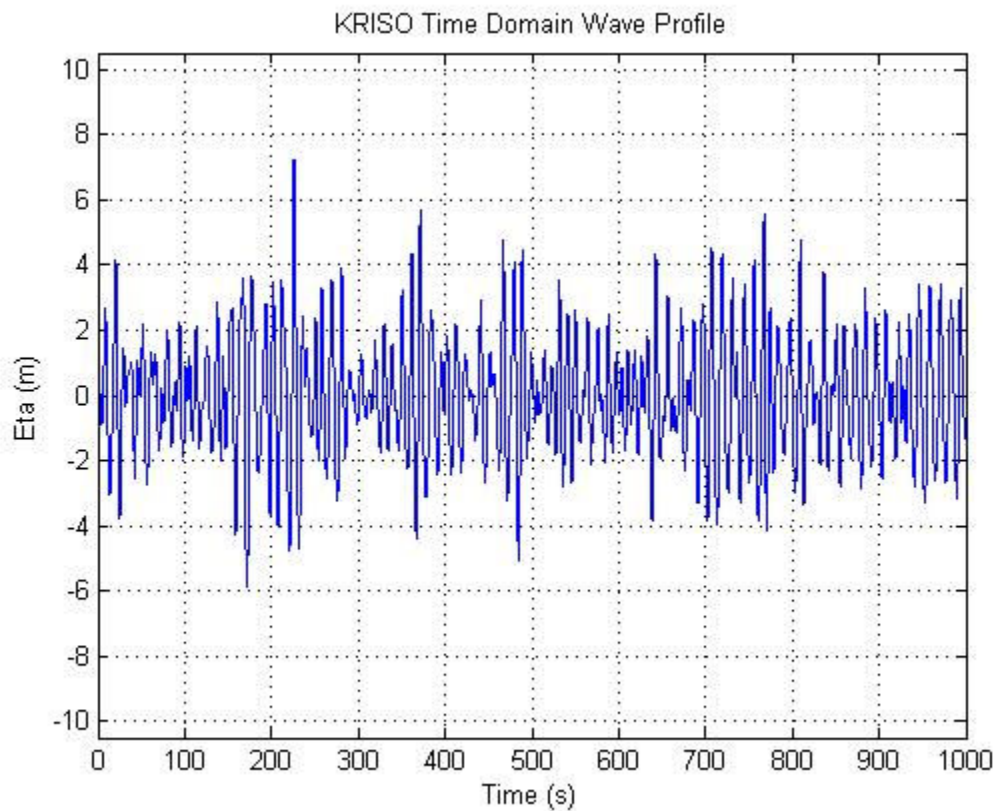


Fig. 20. Wave profile measured amidships for  $H_s = 7\text{ m}$ .



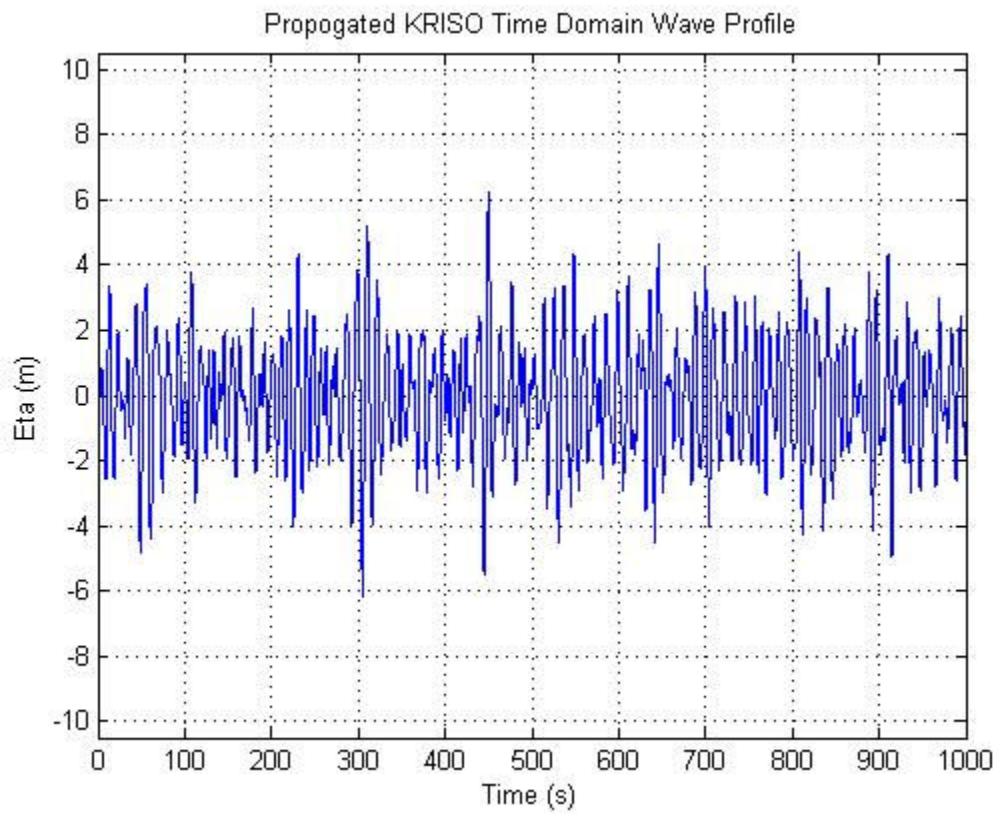


Fig. 21. Wave profile at station 1 for  $H_s = 7$  m.

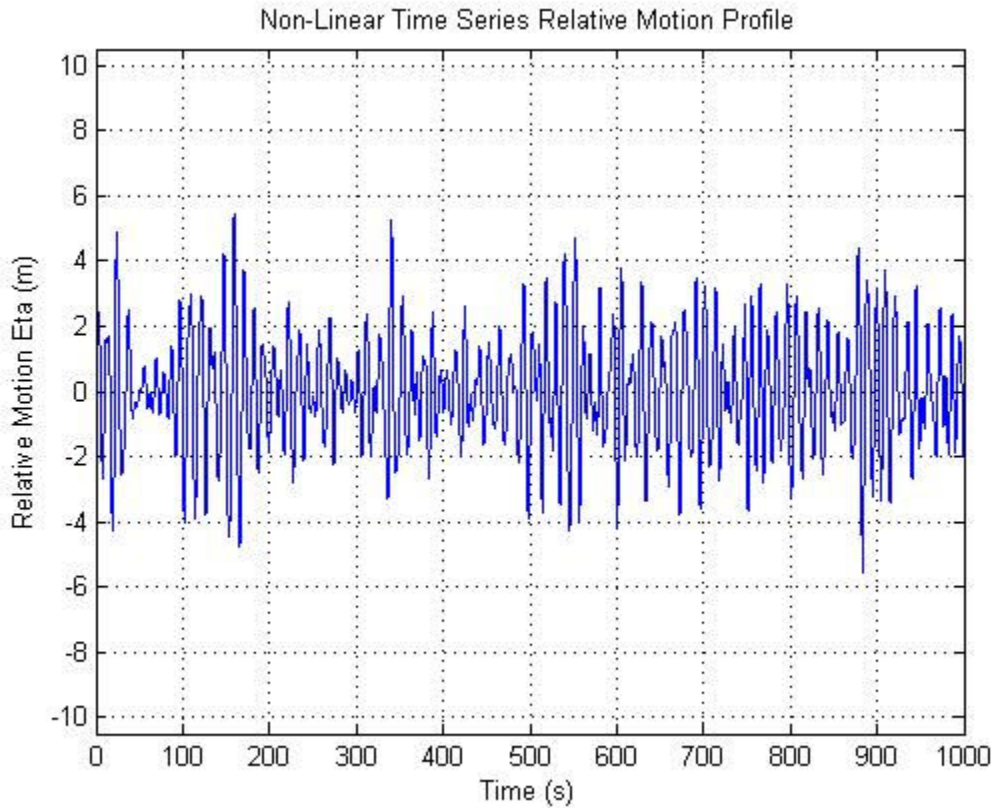


Fig. 22. Relative motion profile at station 1 for  $H_s = 7$  m.

Notice that for  $H_s = 7$  m the probability of exceedence curve for the linear model input wave is lower than that of the nonlinear. This again indicates that with mid level and high significant wave heights, nonlinearities play a significant role in the modeling (see Fig. 23). Like in each of the preceding lower sea states, in the response probability of exceedence curves, the nonlinear is less than that of the linear (see Fig. 24). Again, this indicates that the linear theory is over approximating the nonlinear response.

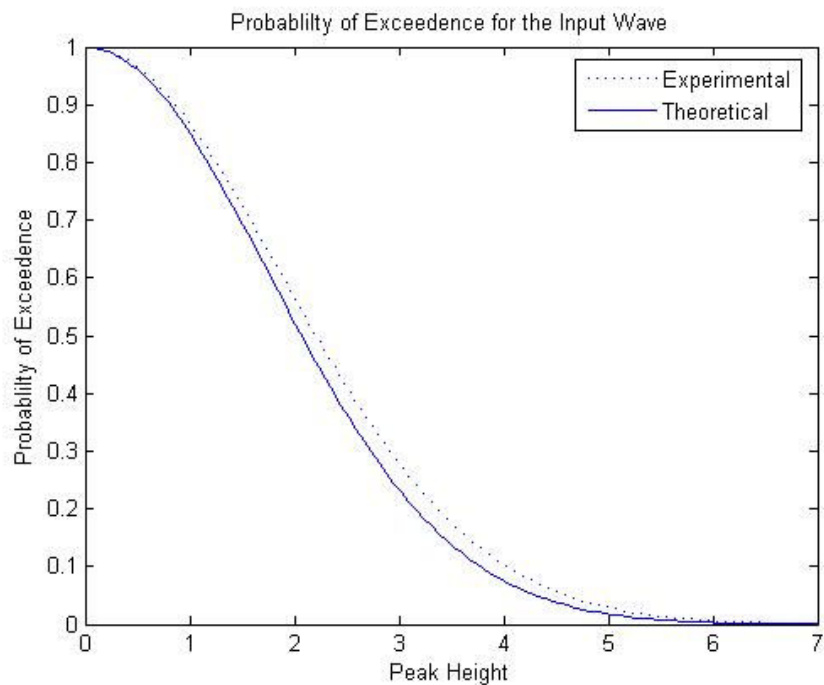


Fig. 23. Comparison of the linear (theoretical) and nonlinear (experimental) input wave for  $H_s = 7$  m.

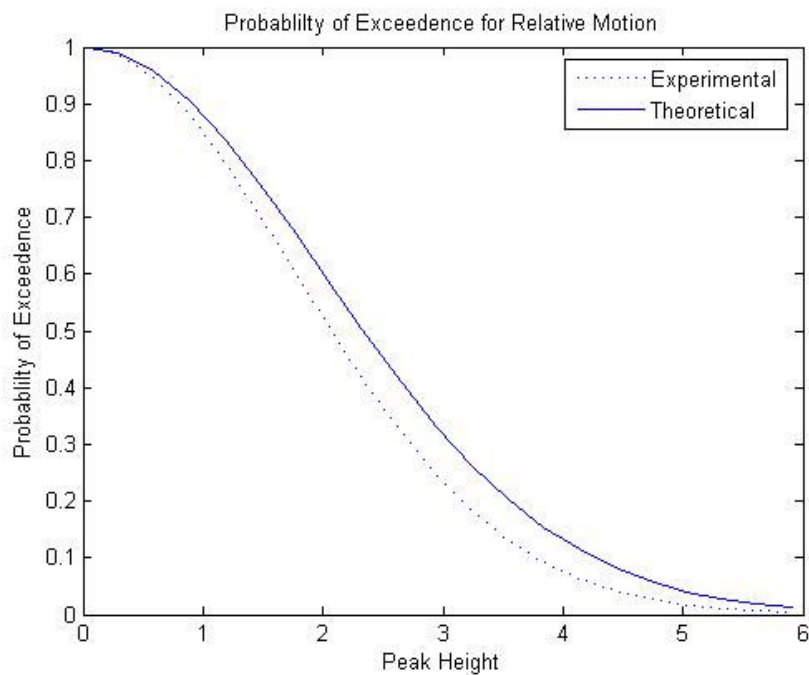


Fig. 24. Comparison of the linear (theoretical) and nonlinear (experimental) relative motion profile for  $H_s = 7$  m.

Case 5:  $H_s = 9$  m

Figure 25 is the unpropagated KRISO data, which is propagated to station 1 in Figure 26. Note the peak of a group in the propagated KRISO data of 6.83 m at 310 s (see Fig. 26). This group then corresponds to a response of 6.83 m at 331 s (see Fig. 27).

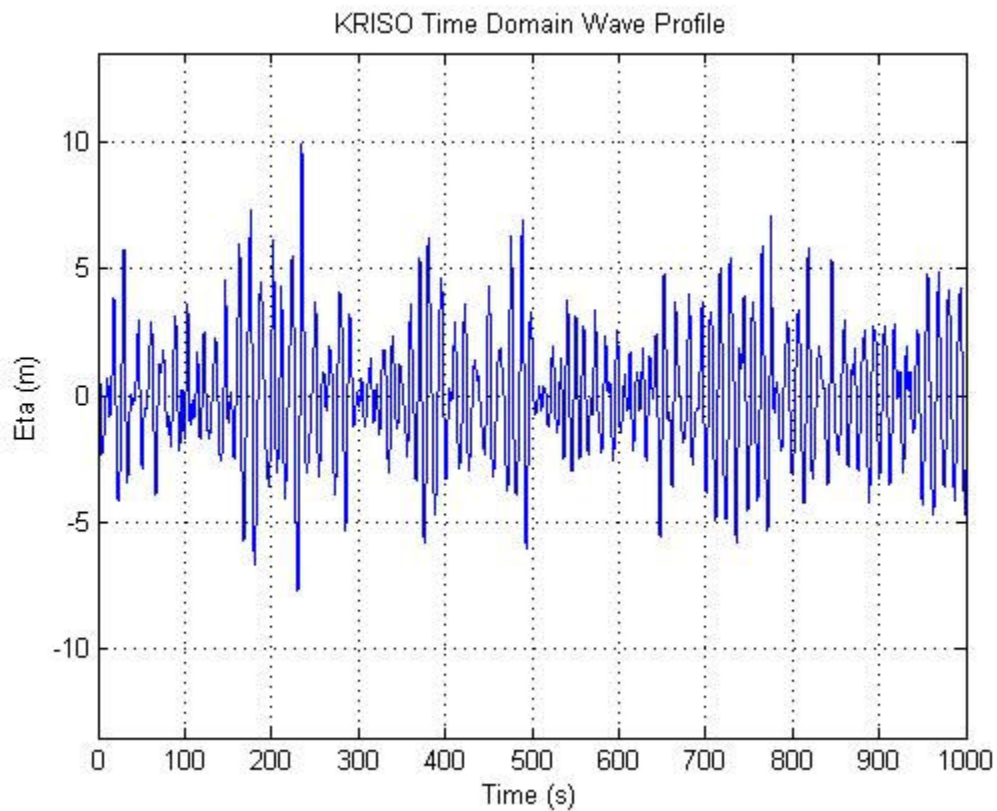


Fig. 25. Wave profile measured amidships for  $H_s = 9$  m.

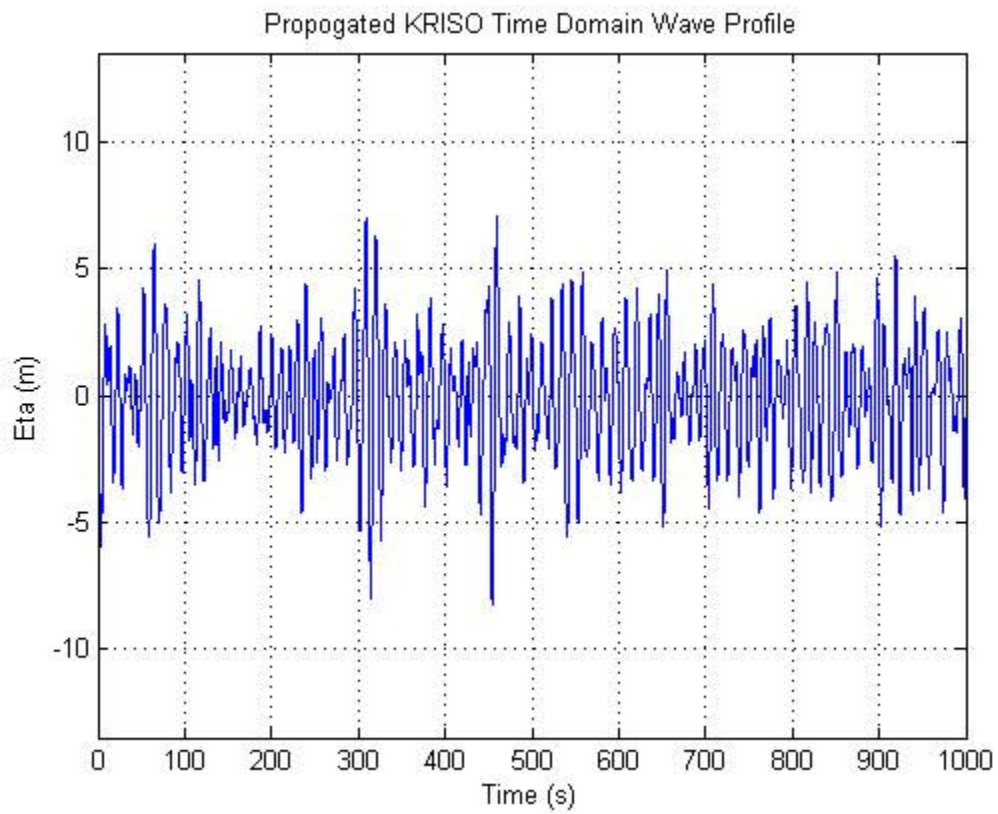


Fig. 26. Wave profile at station 1 for  $H_s = 9\text{m}$ .

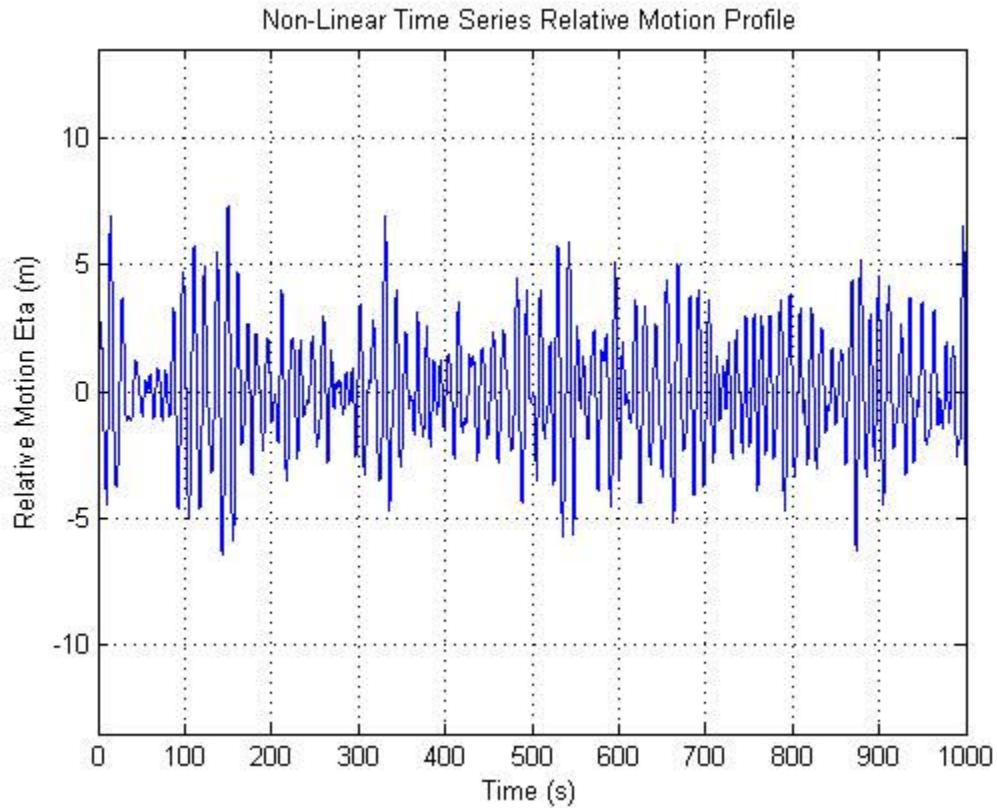


Fig. 27. Relative motion profile at station 1 for  $H_s = 9$  m.

Notice that for  $H_s = 9$  m the probability of exceedence curve for the linear model input wave is lower than that of the nonlinear. This indicates that with higher significant wave heights, nonlinearities play a significant role in the modeling (see Fig. 28). Like in each of the preceding lower sea states, in the response probability of exceedence curves, the nonlinear is less than that of the linear (see Fig. 29). Again, this indicates that the linear theory is over approximating the nonlinear response.

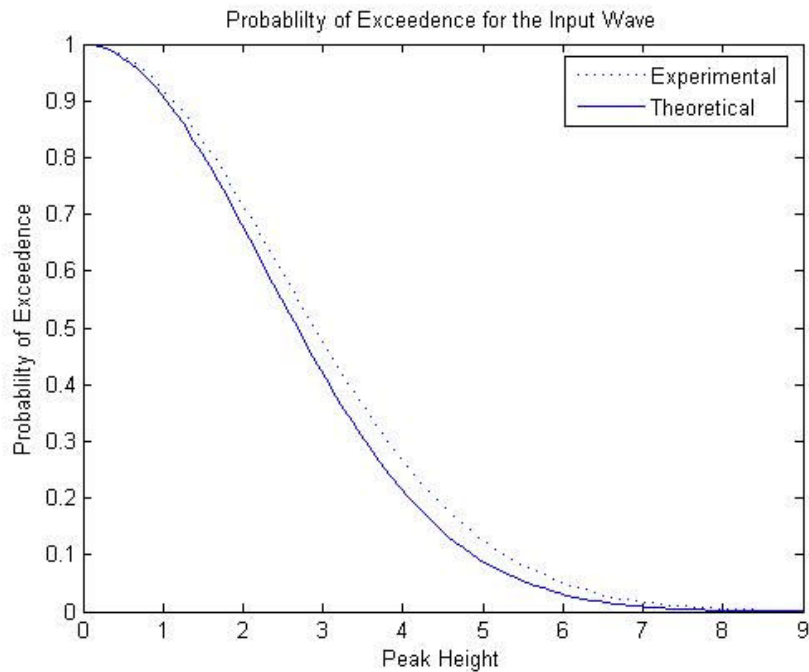


Fig. 28. Comparison of the linear (theoretical) and nonlinear (experimental) input wave for  $H_s = 9$  m.

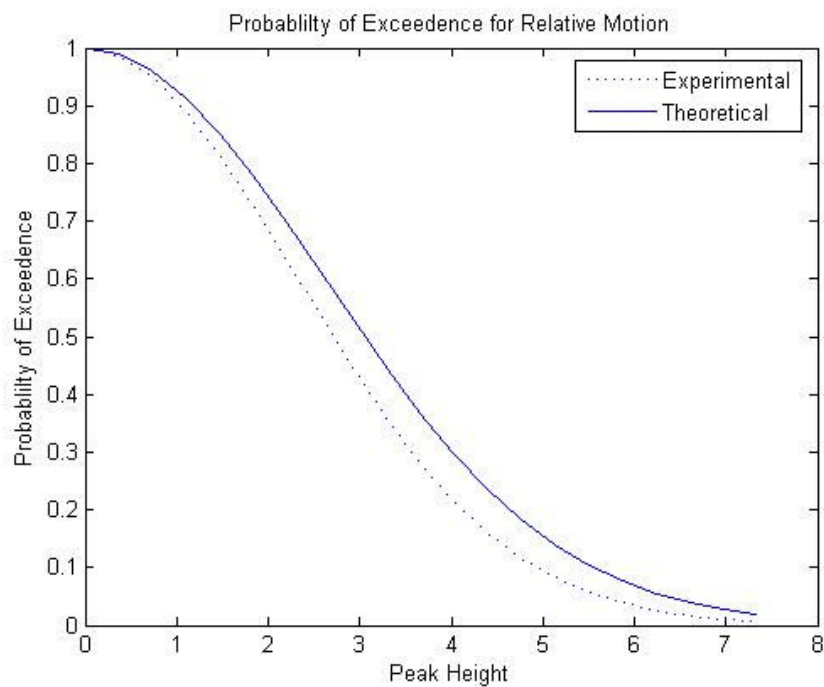


Fig. 29. Comparison of the linear (theoretical) and nonlinear (experimental) relative motion profile for  $H_s = 9$  m.

Case 1:  $H_s = 11$  m

Figure 30 is the unpropagated KRISO data, which is propagated to station 1 in Figure 31. Note the peak of a group in the propagated KRISO data of 7.21 m at 308 s (see Fig. 31). This group then corresponds to a response of 7.29 m at 333 s (see Fig. 32).

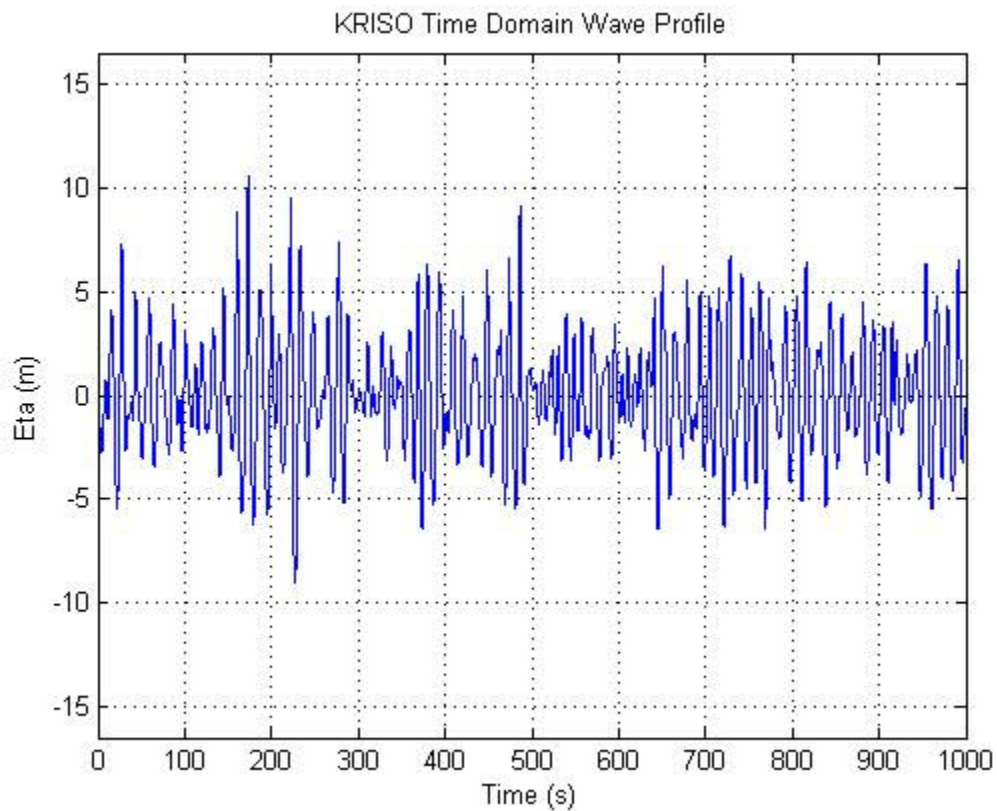


Fig. 30. Wave profile measured amidships for  $H_s = 11$  m.



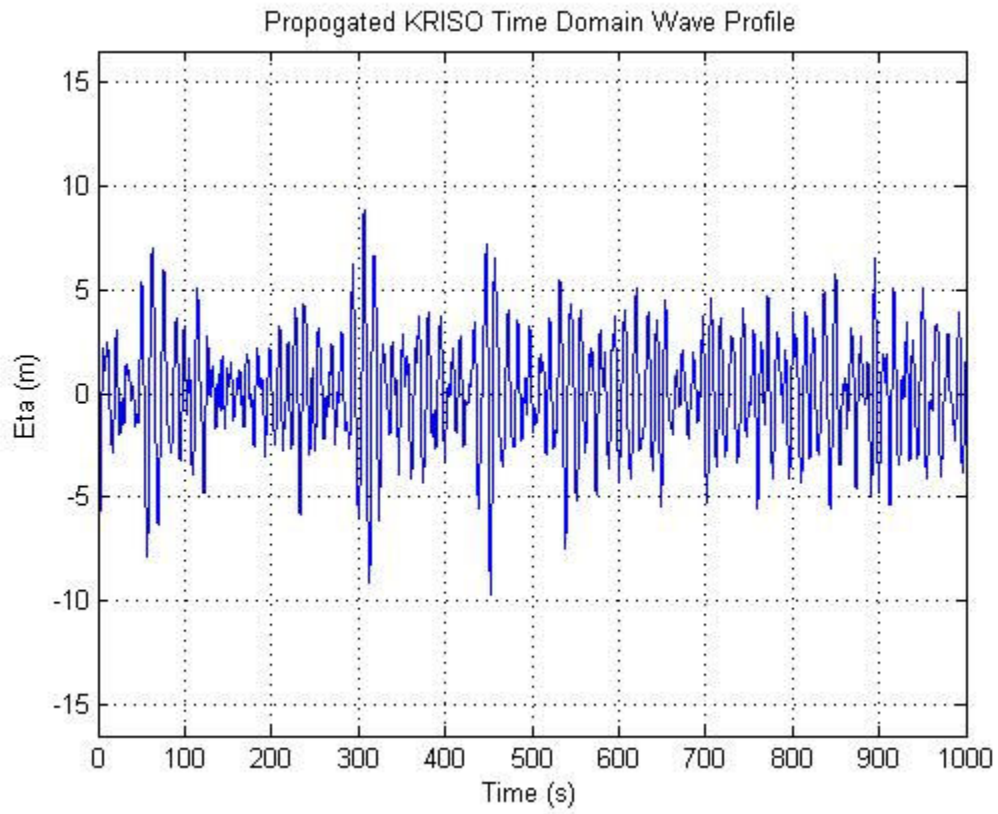


Fig. 31. Wave profile at station 1 for  $H_s = 11$  m.

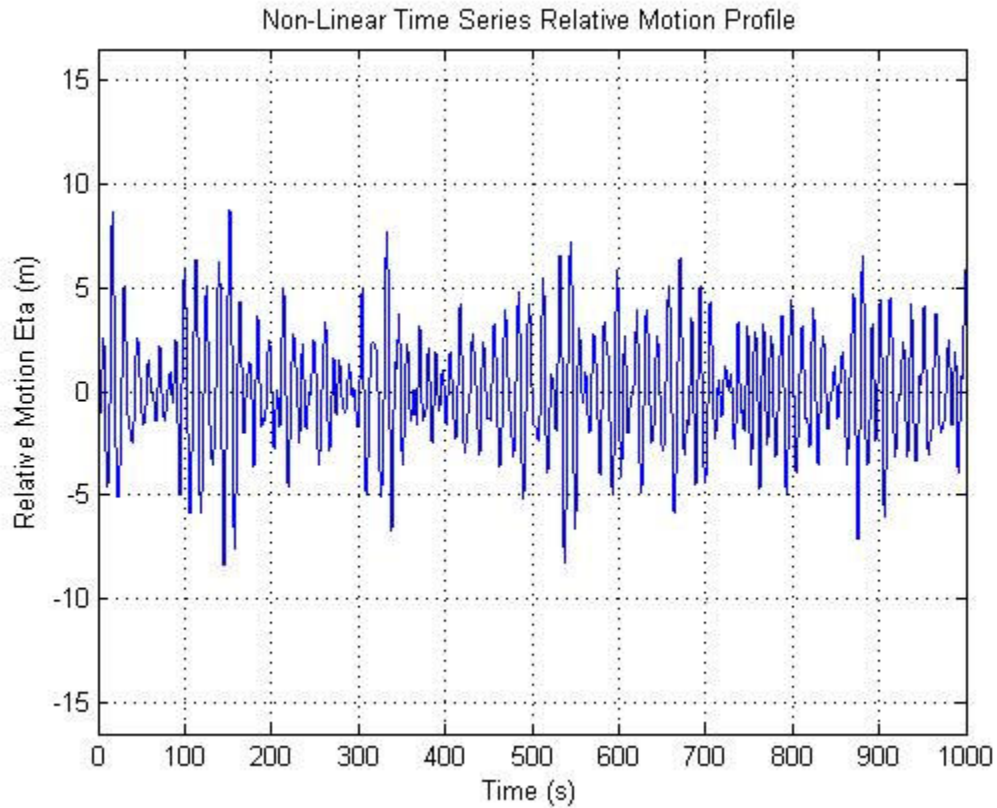


Fig. 32. Relative motion profile at station 1 for  $H_s = 11$  m.

Notice that for  $H_s = 11$  m the probability of exceedence curve for the linear model input wave is lower than that of the nonlinear. This indicates that with higher significant wave heights, nonlinearities play a significant role in the modeling (see Fig. 33). Like in each of the preceding lower sea states, in the response probability of exceedence curves, the nonlinear is less than that of the linear (see Fig. 34). Again, this indicates that the linear theory is over approximating the nonlinear response.

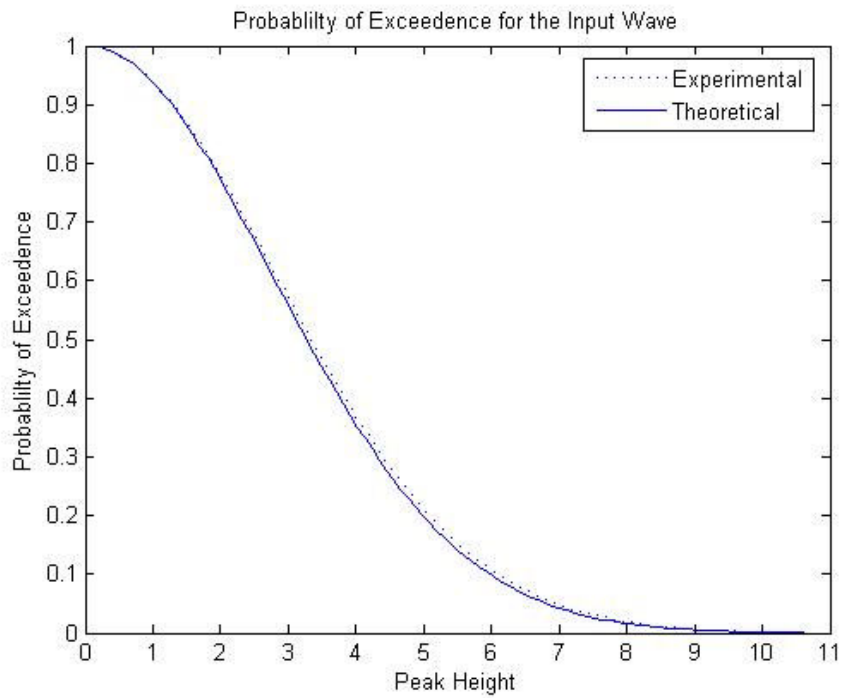


Fig. 33. Comparison of the linear (theoretical) and nonlinear (experimental) input wave for  $H_s = 11$  m.

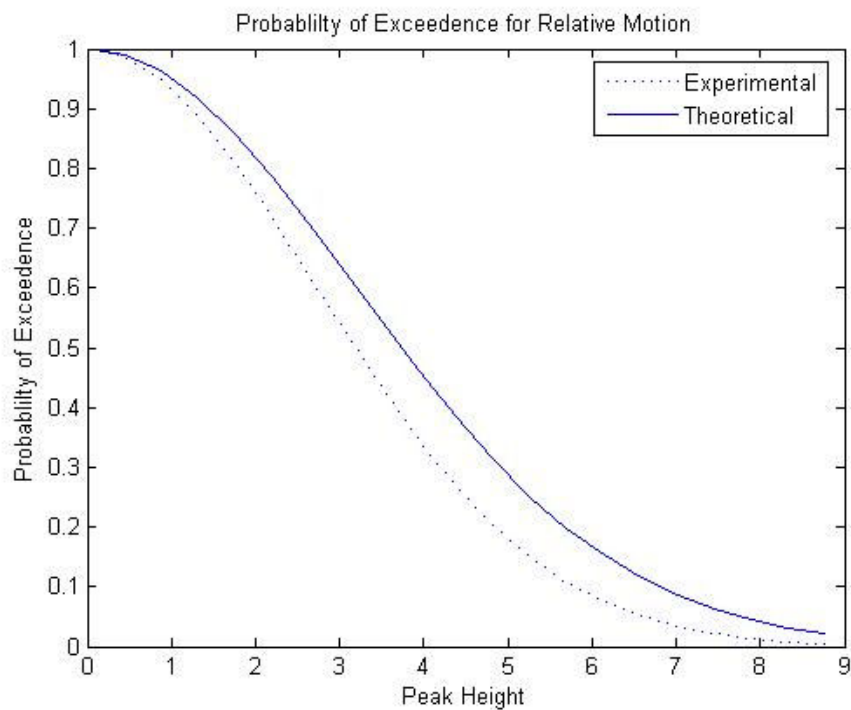


Fig. 34. Comparison of the linear (theoretical) and nonlinear (experimental) relative motion profile for  $H_s = 11$  m.

## CONCLUSIONS

Historically the motion of ships in response to varying sea states has been performed linearly in the frequency domain. These analyses, by their linear nature were not able to handle the nonlinear effects of real world wave. The current study continues the study of a time domain analysis by processing nonlinear data with a linear system. By performing a Rayleigh most probable maximum analysis on the data sets the result is a more accurate response that indicates the presence of nonlinearities, and that the disparity between the linear and nonlinear methods increases as significant wave height increase (see Fig. 35). The Rayleigh most probable maximum is defined by:

$$\hat{a}_N = \sqrt{2 \ln N} \sqrt{m_0} \quad (20)$$

where:

$$\begin{aligned} \hat{a}_N &= \text{most probable maximum} \\ N &= 1000/T_z \\ T_z &= \text{zero crossing period of the data set} \\ m_0 &= \text{variance} \end{aligned}$$

The results, since they are in the time domain, can then be inspected for the presence of wave groups, and their effects on the motion of the ship.

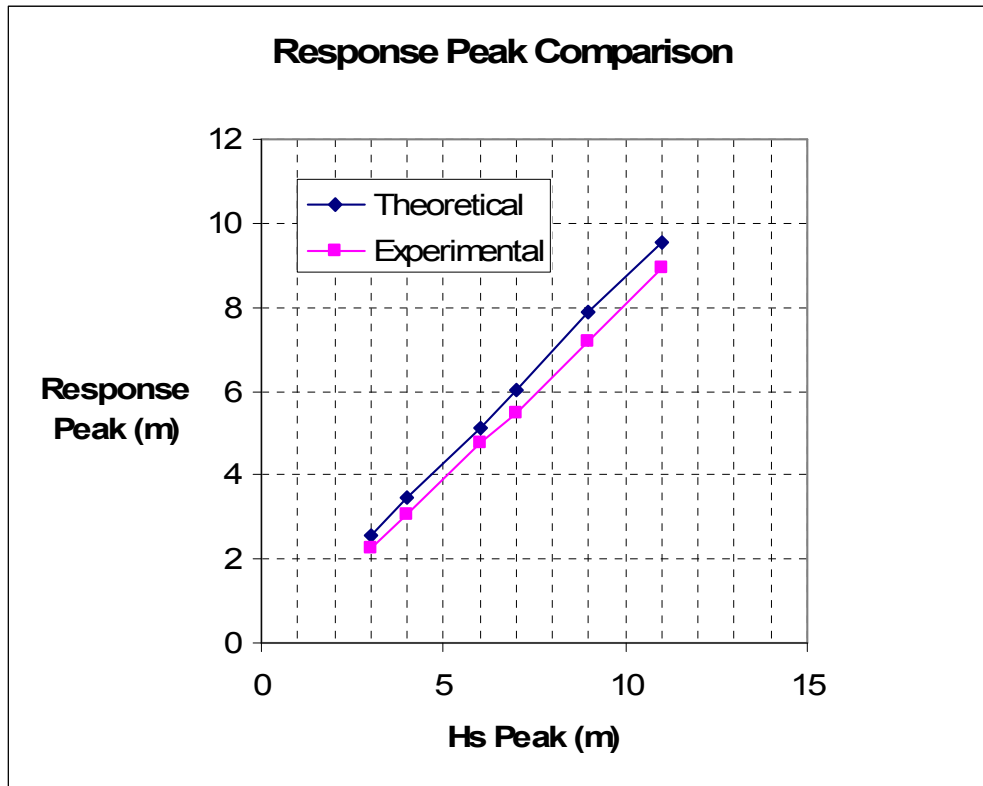


Fig. 35. Most probable peak response for linear (theoretical) and nonlinear (experimental) data.

The present study has indicated that by studying a more accurate set of time domain response data, wave groups will have an effect on the motion of the ship. For each of six sea states, wave profile data was measured at the ships midsection. This profile was then propagated to station 1. This propagation process allowed for the inspection of the presence of wave groups. Since the results of the UNIOM model are in the time domain, the relative motion response can also be inspected for group effects. Table 2 shows that there is consistently a response to a wave group in the wave profile 11 to 49 seconds after the wave group hits the hull, and that this response is consistent with the RAO (response height/wave height).

Table 2  
Response due wave group time lag and comparison to wave height

Hs (m)	Peak Time (s)		Time Lag (s)	Wave Height (m)	Response Height (m)	Response Height/Wave Height
	Wave	Response				
3	316	327	11	1.42	1.89	1.33
	460	483	23	2.88	1.48	0.51
	827	866	39	2.24	2.22	0.99
4	466	477	11	3.00	2.86	0.95
	835	860	25	3.00	2.86	0.95
6	318	330	12	4.47	4.61	1.03
7	310	340	30	5.20	5.23	1.01
9	310	331	21	6.83	6.83	1.00
11	308	333	25	7.21	7.29	1.01

Furthermore, this study implies that ship design may be modified in the future. The results of this study confirm the results generated by Adil in 2004, that showed by using the UNIOM model, the necessary available freeboard for seaward vessels is less than that necessary with a design based on the linear energy spectral method. The lower relative motion response shown by the current study also indicates that since vertical motion of the hull will be less, the design loads for slamming would also be less. Both of these phenomena would mean lower construction costs for ocean vessels. Lastly this study indicates that the effects of wave groups cannot be ignored, however these results are by no means exhaustive. This preliminary study merely indicates that wave group effects cannot be denied. The onus on future studies is to discover the detailed effects these groups have on the response motions of ships.

## REFERENCES

Adil, A., 2004. Simulation of Ship Motion and Deck-Wetting Due to Steep Random Seas. Masters Thesis. Ocean Engineering Program, Civil Engineering Department, Texas A&M University, College Station, TX.

Cummins, W.E., 1973. Pathologies of the Transfer Functions. Naval Ship Research and Development Center, Bethesda, MD.

Dalzell, J., 1962. Some Further Experiments on the Application of Linear Superposition Techniques to the Responses of a Destroyer Model in Extreme Irregular Long-Crested Seas. Report 918. Stevens Institute of Technology, Hoboken, NJ.

Dalzell, J., 1982. An Investigation of the Applicability of the Third Degree Functional Polynomial Model to Non-Linear Ship Motion Problems. Report SIT-DL-82-9-2275. Stevens Institute of Technology. Hoboken, NJ.

ITTC, Report on Seakeeping Committee, 1978. In: Proceedings. 15<sup>th</sup> International Towing Tank Conference, The Hague, Netherlands.

Kim, C.H., Chou Frank S., Tein, D., 1980. Motions and Hydrodynamic Loads of a Ship Advancing in Oblique Waves. Society of Naval Architects and Marine Engineers Transactions 88, 225-256.

Lee, W.T. and Bales, S.L., 1980. A Modified JONSWAP Spectrum Only on Wave Height and Period. Report DTNSRDC/SPD-0918-01. David W. Taylor Naval Ship Research and Development Center. Bethesda, MD.

Tupper, E., 1996. Introduction to Naval Architecture. Reed Educational and Professional Publishing Ltd., The Society of Naval Architects and Marine Engineers, Jersey City, NJ, 108-110.



## APPENDIX A

### Matlab Code used to process the KRISO data

```

%*****
%Compare Theoretical and Experimental RAO's
%Designed by : Jeff Richer,
%Ocean Engineering, Texas A&M University
%College Station, Tx. 77843-3136
%
%Latest Update: 14 August 2005
%*****

format long
clear;
clc;
tic;
close all
clear all

%*****
%Enter The KRISO Data
%
%timescale - converts data time from model to prototype
%
%periodscale - determines what fraction of Kriko data used (i.e.
%periodscale = 3 uses 1/3 of the total Kriko data points)
%heightscale - scales the hs of the raw kriko data to the from model to
%prototype
%
%h - model depth of the KRISO data
%L - Length (in meters) of the Ship
%*****

Hsig=11
Tchar=11.26
Tp=13.37
gam=2.5

timescale=7.41;
heightscale=1.82
periodscale=1.75

h=550;
L=175
x=L/2

smoothparameter=200

%*****
%Load the KRISO (non-linear) Data from Raw Data Files and Define the Time

```

```

%Domain Parameters
%*****

%kriso=load('Z:\Jeff\Research\Rawdata\MATLABKriso\Result.043');
kriso=load('Result.028');
krisoprop=load('Prop028.out')
krisolimit=length(kriso)/periodscale;
t=kriso(1:krisolimit,1)*timescale;
elev=kriso(1:krisolimit,2)/heightscale;
propelev=krisoprop(1:krisolimit,2)/heightscale;
dt=t(3)-t(2);
fs=1/dt;
tmax=krisolimit*dt;
xmax=krisolimit*dt;
T=max(t)/60 %minutes

%*****
%Plot the Original KRISO Wave Profile from Time Series Data
%*****

figure(1)
plot(t(1:length(t)),elev(1:length(t)))
axis([0 1000 -(Hsig+Hsig/2) (Hsig+Hsig/2)])
grid on
title('KRISO Time Domain Wave Profile')
xlabel('Time (s)')
ylabel ('Eta (m)')

figure(2)
plot(t(1:length(t)),propelev(1:length(t)))
axis([0 1000 -(Hsig+Hsig/2) (Hsig+Hsig/2)])
grid on
title('Propogated KRISO Time Domain Wave Profile')
xlabel('Time (s)')
ylabel ('Eta (m)')

%*****
%Generate the Amplitude Density Spectrum using the "FOURIERAMPSPECTRUM"
%and "WAVENUMBECELERITY" Subroutines
%*****

[f0,w0,A0,phase0] = FOURIERAMPSPECTRUM(t,elev);
dw=(w0(3)-w0(2));
A22=A0/dw;
for n=1:1:length(w0)
    [k(n),C(n)] = WAVENUMBECELERITY(w0(n),h);
end
w0=w0(70:518)
A0=A0(70:518)
phase0=phase0(70:518)
U0=(A0.^2)/(2*dw);

% figure(2)
% subplot(2,1,1)

```

```

% plot(w0,A22)
% grid on
% title('KRISO Data Amplitude Density Spectrum')
% xlabel('Omega')
% ylabel ('Amplitude Density')
% subplot(2,1,2)
% plot(w0,phase0)
% grid on
% xlabel('Omega')
% ylabel ('Phase')

% figure(3)
% plot(w0,U0)
% % axis([0 (Hsig) 0 (10*Hsig)])
% xlabel('Omega')
% ylabel('U(Omega)')
% title('Energy Density Spectrum')

% *****
%Load RAO's
% *****

% RAO=load('Z:\Jeff\SHMB5\Recadil\RAO.txt')
RAO=load('RAO.txt');
w=RAO(70:518,1);
hv=RAO(70:518,2);
hvphas=RAO(70:518,3).*(pi/180);
radpit1=RAO(70:518,4);
degpit=RAO(70:518,5);
pitphas=RAO(70:518,6).*(pi/180);
RelRAO=load('RelRAO3');
relmo=RelRAO(70:518,3);
relmophas=RelRAO(70:518,5)

radpit=degpit.*(pi/180);

% figure(4)
% plot(w,hv)
% title('Heave RAO')
% xlabel('Omega')
% ylabel ('Heave RAO (m/m)')
%
% figure(5)
% plot(w,radpit)
% title('Pitch RAO')
% xlabel('Omega')
% ylabel ('Pitch RAO (rad/m)')
%
% figure(6)
% plot(w,relmo)
% title('Relative Motion RAO')
% xlabel('Omega')
% ylabel ('Relative Motion RAO (m/m)')

% *****

```

```
%Generate UNIOM (non-linear)Heave, Pitch and Relative Motions Responses
%*****
```

```
for n=1:1:length(t)/2;
    nonlinhv1=A0.*((hv.*exp(i*(w0.*t(n)-hvphas-phase0))));
    nonlinhv(n)=real(sum(nonlinhv1));
    nonlinpit1=A0.*((radpit.*exp(i*(w0.*t(n)-pitphas-phase0))));
    nonlinpit(n)=real(sum(nonlinpit1));
    nonlinrel1=A0.*((relmo.*exp(i*(w0.*t(n)-relmophas-phase0))));
    nonlinrel(n)=real(sum(nonlinrel1));
end
```

```
% figure(7)
% plot(t(1:length(t)/2),nonlinhv)
% axis([0 1000 -(Hsig+Hsig/2) (Hsig+Hsig/2)])
% grid on
% title('Non-Linear Heave Response')
% xlabel('Time (s)')
% ylabel ('Heave Response (m)')
%
% figure(8)
% plot(t(1:length(t)/2),nonlinpit)
% axis([0 1000 -(Hsig/40) (Hsig/40)])
% grid on
% title('Non-Linear Pitch Response')
% xlabel('Time (s)')
% ylabel ('Pitch Response (m)')
```

```
figure(9)
plot (t(1:(length(t)/2)),nonlinrel)
axis([0 1000 -(Hsig+Hsig/2) (Hsig+Hsig/2)])
grid on
title('Non-Linear Time Series Relative Motion Profile')
xlabel('Time (s)')
ylabel('Relative Motion Eta (m)')
```

```
%*****
%Generate Linear Spectrum for Heave, Pitch and Relative Motion Response
%*****
```

```
% A=173*(Hsig^2)/(Tchar^4)
% B=691/(Tchar^4)
% Uw=((A./w.^5).*exp(-B./w.^4));
```

```
wm=((3/5)^0.25)*(2*pi/Tp);
if w<=wm
    Uw=(5/16).*(Hsig.^2).*(wm.^4).*(w.^-5).*exp(-1.25.*((wm./w).^4)).*(1-
0.287.*log(gam)).*gam.^(exp(-((w-wm).^2)./(2.*(0.07^2).*(wm.^2))));
else
    Uw=(5/16).*(Hsig.^2).*(wm.^4).*(w.^-5).*exp(-1.25.*((wm./w).^4)).*(1-
0.287.*log(gam)).*gam.^(exp(-((w-wm).^2)./(2.*(0.09^2).*(wm.^2))));
end
```

```
Alin=sqrt(2.*Uw.*dw);
```

```

% figure(10)
% plot(w,Uw)
% axis([0 (Hsig) 0 (10*Hsig)])
% xlabel('Omega')
% ylabel('U(Omega)')
% title('JONSWAP Spectrum')

Urh=(hv.^2).*Uw;
Arh=sqrt(2.*Urh.*dw);
Urp=(radpit.^2).*Uw;
Arp=sqrt(2.*Urp.*dw);
Urrel=(relmo.^2).*Uw;
Arrel=sqrt(2.*Urrel.*dw);

% *****
%Statistically Compare Theory and Experiment
% *****

U0s=smooth(U0);
for ss=1:smoothparameter
    U0s=smooth(U0s);
end

varele=var(elev(1:2701))
varelt=trapz(w,Uw)

aw=(0:(max(elev)/100):max(elev));
probe=exp(-(aw.^2)/(2*varele));
probt=exp(-(aw.^2)/(2*varelt));

figure(11)
axis([0 Hsig 0 1])
plot (aw,probe,':')
hold on
xlabel('Peak Height')
ylabel('Probablilty of Exceedence')
title('Probablilty of Exceedence for the Input Wave')
plot (aw,probt,'-')
legend('Experimental','Theoretical',1)
axis([0 Hsig 0 1])

nonlinrel=nonlinrel'
[f0he,w0he,A0he,phase0he] = FOURIERAMPSPECTRUM(t(1:(length(t)/2)),nonlinrel);
dwhe=(w0he(3)-w0he(2));
U0he=(A0he.^2)/(2*dwhe);
% U0hes=smooth(U0he);
% for ss=1:smoothparameter
%    U0hes=smooth(U0hes);
% end

w0he=w0he(70:518);
U0he=U0he(70:518);

```

```
varhe=var(nonlinrel(1:2701))
varht=trapz(w,Urrel)

ah=abs((0:(max(nonlinrel)/20):max(nonlinrel)));
probe=exp(-(ah.^2)/(2*varhe));
probt=exp(-(ah.^2)/(2*varht));

figure(12)
% axis([0 Hsig 0 1])
plot (ah,probe,'-')
hold on
xlabel('Peak Height')
ylabel('Probabilty of Exceedence')
title('Probabilty of Exceedence for Relative Motion')
plot (ah,probt,'-')
legend('Experimental','Theoretical',1)
% axis([0 Hsig 0 1])
```

## VITA

Jeffrey A. Richer

c/o Dr. Robert Randall  
Coastal and Ocean Engineering Division  
Department of Civil Engineering  
Texas A&M University  
3136 TAMU  
College Station, TX 77843-3136

### Education

- M.S., Ocean Engineering, Texas A&M University, December 2005
- B.S. Civil Engineering, Lehigh University, June 1996

### Experience

- Public Works Operations Officer, Naval Mobile Construction Battalion Center, Gulfport, MS, January 2003 – August 2004
- Assistant Resident Officer in Charge of Construction, Naval Air Weapons Station, China Lake, CA, January 2001 – January 2003
- Project Engineer, Kadrmas, Lee and Jackson, Billings, MT, July 1999 – April 2000
- Project Engineer, CTA Architects Engineers, Billings MT, June 1998 – July 1999
- Project Engineer, Pany and Lentz Engineering, Allentown, PA, September 1997 – February 1998
- Site Inspector, Certified Testing Laboratories, Bethlehem, PA, June 1996 – June 1997